Novel *Self-Decorrelation* and *Fractional Self-Decorrelation* Pre-processing Techniques to Enhance the Output SINR of Single-User-Type DS-CDMA Detectors in Blind Space-Time RAKE Receivers

CHEUNG *Shun Keung*

A Thesis Submitted in Partial Fulfillment
of the Requirements for the Degree of
Master of Philosophy
in
Electronic Engineering

July, 2002

應用嶄新的「自分離相關」和「部分自分離相關」處理方法來改善盲空時多徑衰落接收技術

張順強

電子工程課程

哲學碩士論文

2002 年 7 月

Abstract

The novel "Self-Decorrelation" and "Fractional Self-Decorrelation" techniques are herein proposed to enhance the multipath constructive summation capability and the interference rejection capability for the family of maximum-SINR blind space-time DS-CDMA RAKE receivers designed to tackle the near-far problem in DS-CDMA cellular mobile communication.

The "self-decorrelation" technique is used to increase the output SINR in the family of maximum-SINR blind space-time RAKE receivers proposed by Chen, Zoltowski & Ramos [1] and Wong, Lok, Lehnert & Zoltowski [2] with the assumption that the multipath delay spread occupies only a small fraction of the symbol duration, such as in the IS-95 standard. The optimum beamforming weight vector for combining the desired user's multipaths is the largest generalized eigenvector of the matrix pencil pair. The matrix pencil pair is composed of signal-plus-interference-and-noise (S+I+N) space-time correlation matrix and interference-plus-noise (I+N) space-time correlation matrix, which are originally formed by segmenting the post-correlation symbol interval into S+I+N segment and I+N segment respectively.

The proposed "self-decorrelation pre-processing" is the orthogonal projector with respect to the vector space spanned by the desired user's signature sequence and its time-delayed versions up to the duration of a cluster of "fingers" in a symbol interval. After the pre-processing of the received baseband signal, the I+N space-time correlation matrix is formed by using the pre-processing output where the signal-of-interest (SOI) energy is *completely removed* in a

symbol interval. This is a significant step to remove a trace of SOI energy in I+N segment in the original algorithm, which a more accurate I+N space-time correlation matrix is estimated, *without the despreading* process. As a result, the optimum beamforming weight vector for element-space-only [1] beamformer is more accurately estimated.

The proposed "fractional self-decorrelation" pre-processing technique could be applied to the family of maximum-SINR blind space-time RAKE receivers developed by Chen, Zoltowski & Ramos [1] but the multipath fading delay spread could approach the *whole symbol duration.* It is the extension of self-decorrelation pre-processing when the multipath delay spread is no longer assumed to be within a small fraction of the symbol interval. A typical application is in the high-speed data communication for next generation mobile communication.

"Fractional self-decorrelation pre-processing" is the eigen-subspace orthogonal to the vector space spanned by selecting a certain number of largest singular-value column vectors of the column space which is spanned by the desired user's signature sequence and all its time-delayed versions within a symbol duration. This eigen-subspace acts as a projector with *arbitary dimensions*, but should not equal to the full dimension of the vector space spanned by all time samples in a symbol duration. The purpose of the fractional self-decorrelation pre-processing is to remove those desired user's multipaths with *dominant* signal energy at the receivers so that the I+N space-time correlation matrix is formed, with much of the *SOI's dominant energy removed.* The newly estimated element-space beamforming weight vector is more accurate than the original methods developed by Naguib et.al.[3], Liu & Zoltowski [4], Liu & Geraniotis [5] and Luo & Blostein [6].

[1] One of the receiver architectures in the family of receivers in Chen et.al. [1]

論文摘要

本論文的貢獻是建議採用兩種新穎的技術去改善一系列的盲空時處理計劃，本文稱這兩種技術分別爲自分離相關(self-decorrelation)和部分自分離相關(fractional self-decorrelation)前處理技術。這些盲空時處理計劃原本是應用於一個家族的接收器的，而這家族是應用最大信干噪比(SINR)的準則於異步碼分多址(DS-CDMA)多徑衰落的盲空時 RAKE 接收器上來測量它的精測表現，這些接收器利用一系列盲空時處理方法來解決遠近(near-far)問題。本文建議的兩種技術能改善應用於該家族接收器裏應用的盲空時處理計劃，令接收器的輸出信干噪比增加來解決遠近問題。這兩種技術是透過增加多徑建設性疊加的能力和對抗干擾的能力去改善該系列盲空時處理計劃的。

自分離相關技術能應用於 Chen et.al. [1]等作者所提出的一系列多徑衰落的盲空時 RAKE 接收器上，這類接收器的發展是基於一個假設的，多徑時延分佈的時間長度只佔符號時間長度的一小部分。現在流動通訊市場上應用的 CDMA 制式—IS-95 標準就是一個例子。應用了建議的技術後，最佳的發射波束形成權向量仍是原本提出的最大普遍化特徵向量(largest generalized eigenvector)，這向量是從一對矩陣所得到的，這對矩陣分別是信+干+噪(S+I+N)和干+噪(I+N)空時相關矩陣，在 Chen et.al. [1]等作者這一對矩陣原是在同一解擴後的符號時段裏分開兩段不同時段—(S+I+N)時段和(I+N)時段來形成的。

自分離相關技術其實是一個正交投影器，這投影器所形成的子空間是正交於一個子空間，這子空間就是利用指定用戶的擴頻碼和它的時延至多徑時延分佈的向量所展延的。所以，當收集到的基底信號經過自分離相關器處理後，干噪空時相關矩陣可以利用自分離相關器的輸出數據來形成，而不須要用 Chen et.al. [1]等作者所提出的原本方法，這輸出數據的好處是在符號時段裏，指定用戶的信號能量能完全消去，所以干噪空時相關矩陣能更準確的計算出來。

部分自分離相關技術也可應用於 Chen et.al. [1]等作者所建議的一個家族的接收器上，而又不受制於 Chen et.al. [1]等作者所提出的假設，多徑衰落時分佈能平均分佈於整段符號週期。最典型的例子是水聲信號通訊系統。

其實這技術是一個正交特徵子空間，正交於的特徵子空間是從指定用戶擴頻碼和它的時延至整段符號週期的向量裏選出某一數目的最大特徵向量來展延。而這特徵子空間的維數是可以任意的，但不能等於被所有在符號週期內的時間樣本形成的時延向量所展延的空間維數。這種處理技術的目的在於將擁有較多能量的指定用戶的多徑信號消除，從而令到所得的(干+噪)空時相關矩陣和發射波束形成權向量，比 Naguib et.al.[3]; Liu&Zoltowski [4]; Liu&Geraniotis [5]和 Luo&Blostein [6]等作者建議的方法更準確。

Acknowledgments

I would like to thank Dr. Kainam Thomas Wong (ktwong@ieee.org), my supervisor during my first year of thesis research, for permission to use materials in [7] co-authored by Dr.K.T.Wong,myself and others and materials in [8] co-authored by Dr. K. T. Wong and myself.

It has been my privilege to work with both Prof.Pak-Chung Ching (pcching@ee.cuhk.edu.hk) and Prof.Yiu-Tong Chan (ytchan@ee.cuhk.edu.hk or chanyt@rmc.ca), my supervisors in my second year of thesis research. I benefited from their valuable comment, guidance and advice.

As a new comer of Electronic Engineering Department in CUHK, I enjoyed my two-year study in DSP lab. Firstly, I got technical support from our lab technician, Arthur Luk. I learnt a lot from Wai-Kit Lo. It seems to me that he knows everything, for example, he can write complicated programs in all existing programming languages, technical skills in hardware, software and networking, and he knows how to pay less tax. Originally, I knew nothing about PC games and comic books. I gained much useful knowledge about them from Ka-Man Law, Wing-Nin Choi, Wai Lau and Yiu-Wing Wong, especially the selling price of Game Boy and which football team is competitive in a popular PC game called "Winning Eleven". Also, Kin-Fai To taught me how to use a software "WinEdt" to type this thesis in latex.

Moreover, Sze-Wan Wu taught me how to type Chinese Character. I knew the assessment process of applying for a clerk position in CUHK from her. I would also like to thank Ka-Yan Kwan for her advice and guidance during my

study. She taught me how to add a printer driver in a PC when I first came to DSP lab. Also, Hiu-Sing Lam told me a lot about the recruitment process of an assistant officer in ICAC, which the detailed information of all family members are needed to be submitted.

I sincerely thank Yujia Li, Chen Yang, Yao Qian and Ben-Rong Chen for their help to train my Mandarin speaking. I am grateful to Chin-Hang Yau, Patgi Kam, Lai-Yin Ngan and Wan Lam for their giving me lot of fun time. I am glad that Wing-Kin Ma invited me to participate his wedding dinner and Kei-Dzoen Wong's borrowing me his digital camera for taking photos.

Last but not least, I wish to express my deep gratitude to my mother, Leng-Won Yee and my sister, Lai-Mei Cheung for their kind concern and support during my 2-year MPhil study.

Contents

List of Figures

List of Tables

Chapter 1

Introduction

1.1 The Problem

Nowadays, wireless communication is one of the major parts of communication among fiber optics and computer communication network. It is widely used in our daily life such as radio/TV broadcast, cellular mobile phones and GPS (global positioning system). Also, wireless communication is widely applied in the military such as in acoustic underwater communication and satellite communication.

The research in wireless communication is hence rapidly developed. There are several research areas in wireless communication including multiple access techniques, wireless networking design, fading channel modelling, source coding, channel error-correcting codes, information theory, diversity and equalization.

There are three main kinds of multiple access methods including FDMA (frequency division multiple access), TDMA (time division multiple access) and CDMA (code division multiple access).

Multiple access techniques used in wireless communication is to share a finite amount of radio spectrum with many mobile phone users simultaneously. This is an advantage because the system capacity will be fully utilized assuming that acceptable reception quality is maintained. In a densely populated region,

the number of potential concurrent mobile phone users is large. The increase in system capacity will accommodate more users and avoid blocked calls at busy period. For commercial wireless communication system operators, increasing the capability to serve more mobile phone users will lower its operation cost and hence make a greater profit. So, multiple access schemes are necessary issues in multi-user wireless communication system with limited radio spectrum.

In the thesis, we focus on CDMA since this is a state-of-the-art multiple access technique used in 3G(third generation) cellular mobile communication in the near future and it is an important technique widely used in military communication for its better security due to the low probability of intercept and anti-jamming capability.

1.2 Overview of CDMA

CDMA is one of the multiple access techniques among FDMA and TDMA. Each user in a cell [1] is assigned to a codeword or signature sequence. This codeword is usually generated by a pseudo-noise sequence generator. The generated pseudo-noise sequence has some important characteristics, for example, there are very low correlation between all the shifted versions of the same sequence and very low cross-correlation among the sequences assigned to each user. These two properties are to lower the interfering effect caused by the multipath fading and the other multiple access interfering sources. The pseudo-noise sequence will then map to some waveforms. For example, in non-return-to-zero (NRZ) line coding scheme, bits '1' and '0' are mapped to a pair of anti-podal rectangular pulses. The signature sequence will result in a noise-like waveform after the NRZ pulse mapping. The resulting waveform is called a spreading signal. This spreading signal is then used to modulate our

[1] A small geographic area with a base station monitoring a group of radio channels.

information-bearing baseband signal, which is called Spread Spectrum modulation technique. The resulting spread spectrum baseband signal will be a noise-like signal with approximate flat-top power spectral density, which is like the power spectral density of a white Gaussian noise random process. Therefore, each user in the same cell might manipulate other multiple access interfering sources as additive noise with flat-top power spectral density.
We purposely make the transmission bandwidth a several orders of magnitude larger than the information data transmission rate. Though it seems that spread spectrum is not bandwidth efficient when only one user is in the system. However, it will be bandwidth efficient when multiple users share the same frequency spectrum by using spread spectrum modulation technique, assuming that each user does not interfere with each other.
Therefore, in DS-CDMA system, the transmitted signal of each user is modulated by a unique spreading signal controlled by a pseudo-noise sequence. It allows multiple users transmitting message signals occupying the same radio spectrum at the same time.

1.3 Problems Encountered in Direct-Sequence (DS)CDMA

1.3.1 Multipath Fading Scenario in DS-CDMA Cellular Mobile Communication

Multipath fading scenario exists in the cellular mobile communication. When a mobile phone user transmits its information-bearing signal, this signal will become several multipaths when it arrives at the base-station since there are often some reflecting objects and scatterers between the base-station and the mobile phone users. This constantly changing channel environment will cause distortion of signal amplitude, phase and multipath propagation delay spread.

Since multipath propagation delay lengthens the arrival time of the transmitted signal, inter-symbol interference will often occur. Therefore, several amplitude-attenuated, time-delayed and phase-shifted replicas of the original transmitted signal will arrive at the base-station.

In DS-CDMA, there are multiple active users concurrently sharing the same radio spectrum. Each user will have its own series of amplitude-attenuated, phase-shifted and time-delayed multipath signals arriving at the base-station. Hence, the desired user's transmitted signal, the other multiple access users' (multiple access interference, heretofore designated as MAI) transmitted signal together with the additive noise produced by the base-station receivers' hardware exist in the CDMA communication channel.

Therefore, at the base-station receiver, it needs to sum the desired user's multipath signal constructively and simultaneously suppress the multiple access interfering sources' multipath signal.

1.3.2 Near-Far Problem

Originally, each user in DS-CDMA system is assigned to a signature sequence which is orthogonal to each other. After the spread spectrum modulation of each user's transmitted baseband signal, the orthogonality is preserved. However, due to the multipath fading , the orthogonality is lost. The received multipath signals of the desired user at the base-station are correlated with those of MAI. Therefore, each user in DS-CDMA system interferes with each other. The desired user could not manipulate the MAI as additive white noise alone since there is non-zero cross-correlation between the received multipath signals of each user, making worse reception quality, especailly when the received signal powers are varied distinctively at the base-station receiver. For example, the desired user who is very near to the base-station transmits its signal to the base-station and at the same time, there is a MAI far away from

the base-station near the boundary of the cell transmits its message signal. The received multipath signals' power varies a lot. The user near the base-station will result in a much higher signal power received at the base-station while the user at the boundary of the cell will have a weaker signal power arriving at the base-station. Since there is a non-zero cross-correlation among the multipath signals of the desired user and those of the MAI, the user with a higher multipath signals' power received at the base-station will be dominant. This causes a strong interfering effect to the other users within the same cell. In other words, there is an irreducible error floor to each active user in the DS-CDMA system at the base-station receiver. So, optimal power allocation scheme to each active user is necessary to equalize the received signal power levels at the base-station to avoid the dominant interfering effect.

"Near-Far " problem is inherent in DS-CDMA system because of the non-zero cross correlation among all the multipath signals of all users and the unequalized received signal powers due to the various distances between the users and the base-station. Hence, at the base-station receiver, the unequal received signal power of all users will result in uncontrolled and severe interfering effect to each user in the system.

1.4 Delimitation and Significance of the Thesis

This thesis research focuses on improving the bit error rate(BER) performance of a class of family of blind space-time RAKE receivers with single-user-type detectors by deriving a more accurately estimated beamforming weights which is applied to the post-despreaded baseband data at each antenna element. This is equivalent to solving the aforementioned near-far problem so that the interfering effect caused by both correlated multipaths of the desired user and

those of MAI ;and unequalized received signal powers due to the distinctive distances between each user and the base-station, will be decreased.

At the base-station, if there is only one antenna, the conventional RAKE receiver could only apply some weighting coefficients on the received post-despreaded signal to give out the increased signal-to-interference-plus-noise ratio (SINR) baseband data output for later bit decision making. However, if there is an array of antenna, reception diversity will increase. This means that we could choose and sum up those high-SINR fingers constructively from different post-despreaded baseband data at each antenna element in the array. Each finger in the post-despreaded baseband data is corresponding to one resolvable time-delayed multipath signal of the desired user. This task could be done by applying some weighting coefficients across both spatial and temporal fingers in the post-despreaded baseband data at each antenna element. The resulting weighted baseband data output will have its SINR increased to lower the bit error rate at the bit decision making process.

This family of receivers is "blind" because the receiver does not need to know the desired user's multipath signals' direction of arrival, arrival time delay, attenuated amplitude, phase and polarization state distortions. In conventional RAKE receiver, the above information is necessary to sum all the desired user' multipath signals constructively and reject strong multiple access interference. This information is usually given to the receiver at the base-station through the pilot channel such as in the IS-95 standard. This is an disadvantage because the extra bandwidth will be occupied by sending training sequence between the base-station and the mobile phone users.

With a more accurately estimated beamforming weight vector, we could use it to form a beam pattern pointing a direct gain towards the desired user's location while nulling out the direction of arrival of the multiple access interference. This will provide a spatial reception diversity to the receiver.

In short, this thesis research proposes two novel techniques, which are used

to improve the performance of the family of blind space-time RAKE receivers in Chen et.al. [1] with single-user-type detectors applied. The derived beamforming weight vector will then be more accurately estimated ;hence the two techniques significantly increase the beamformer's output SINR and hence the irreducible error floor, due to the non-zero cross-correlations among the multipaths of all users, will be removed and the bit error rate will be decreased.

1.5 Summary

Two new techniques are proposed in the thesis.They are named "self-decorrelation" and "fractional self-decorrelation" techniques which aim to remove the signal of interest (SOI) energy completely in the I+N data group but with no excessive distortion. Hence, a more accurate I+N spatial (Naguib et.al.[3]) or space-time (Chen et.al.[1]) correlation matrix is formed for later generalized eigen-decomposition procedure for estimating optimum beamforming weight vector. These two techniques significantly improve the performance of the family of maximum-SINR blind space-time DS-CDMA RAKE receivers developed by Wong, Lok, Lehnert & Zoltowski [2] and Chen,Zoltowski and Ramos [1]. The proposed "fractional self-decorrelation" pre-processing has a comparable performance with the interference cancellation methods developed in Liu & Geraniotis [5] and Luo & Blostein [6], but without the need to double the channel capacity occupied by each multiple access user in the cell. It has a notable improvement compared with Naguib et.al. [3] where a significant SOI energy exists in the I+N data group. It is also not constrained by the assumption that the multipath delay spread is within a small fraction of a symbol duration, as in Chen et.al. [1] and Wong et.al. [2].

1.6 Scope of the Thesis

Chapter 2 will be divided into two sections. Section 2.1 describes the space-time data model in DS-CDMA. Section 2.2 includes the literature review of a class of signal processing schemes applied at the family of "blind" space-time RAKE receivers and the weakness in those algorithms.

Chapter 3 will describe how the "self-decorrelation" technique is used to increase the output SINR in the family of receiver structures developed by Chen et. al. [1]. The simulation results of the proposed technique used in the Element-Space-Only (ESO) RAKE receiver [2] will be shown.

Chapter 4 will explain how the "fractional self-decorrelation" technique is used to improve the performance of signal processing schemes without the assumption made by Wong et.al.[2]. The simulation results comparing the schemes of Naguib et.al.[3], Liu & Geraniotis [5] and Luo & Blostein [6] with the proposed scheme will be included.

Chapter 5 includes the complexity analysis and the detailed schematics of the two proposed techniques applied in the Element-Space-Only (ESO) RAKE receiver.

Chapter 6 discusses the conclusion and summary of the contribution of the thesis. Future work will also be included.

[2]ESO RAKE receiver is one of the receiver structures in the family of receivers developed in Chen et.al.[1].

Chapter 2

Literature Review of Blind Space-Time Processing in a wireless CDMA Receiver

2.1 General Background Information

2.1.1 Time Model of K-User Chip-Synchronous CDMA

There are two basic synchronous CDMA channel models by Verdu [13]. They are continuous-time and discrete-time K-user channel models. Basic continuous-time synchronous CDMA K-user channel model is shown below.

$$y(t) = \sum_{k=1}^{K} A_k b_k s_k(t) + \sigma n(t), t \in [0, T] \tag{2.1}$$

The notation of the above equation is defined as follows. T is the inverse of the data rate. $s_k(t)$ is the deterministic signature waveform assigned to the kth user, with unit energy. The signature waveforms are assumed to be zero outside the interval $[0, T]$, and hence, without inter-symbol interference. A_k is the received amplitude of the kth user's signal. $b_k \in \{-1, +1\}$ is the bit transmitted by kth user. $n(t)$ is white Gaussian noise with unit power spectral density. Variable t symbolizes the continuous time index.

This fundamental equation models the K users simultaneously sharing the same channel frequency spectrum (co-channel users) in the continuous time case. We assume the transmitters and the receivers know the clock information of each other and there is no time delay of the signal transmission path between the transmitters and the receivers. Also, each user is assumed to have one transmission path. The corrupting source to the transmitted signal is only the Additive White Gaussian Noise (AWGN) without the effect of dispersive multipath fading. Below is the counterpart in the discrete-time case.

$$y[i] = \sum_{k=1}^{K} A_k b_k s_k[i] + \sigma n[i], i \in \mathbb{Z}, \text{a set of intergers} \tag{2.2}$$

We assume the sampling rate is 1 sample per unit time for mathematical simplicity. Variable i represents the discrete time index.

2.1.2 Dispersive Channel Modelling

For the mobile radio propagation models, there are two types, *large-scale* path loss model and *small-scale* multipath fading model described in Rappaport [14] and Cheng [15].

In the small-scale fading model, the two common types are flat fading and frequency-selective fading. The flat fading channel model is used if the bandwidth of transmitted signal is narrow compared with the coherent channel bandwidth. In contrast, it is appropriate to use the frequency-selective fading channel if the bandwidth of the transmitted signal is wide compared with the coherent bandwidth of the wireless channel. The following gives the two Rappaport [14] models.

(a)Flat fading channel model described in Rappaport[14] and Cheng's lecture notes [15]:

Multipath fading channel gain $a(t)$ could be modelled as:

$$a(t) = a_I(t) + j a_Q(t) \tag{2.3}$$

where $a_I(t)$ and $a_Q(t)$ follow Gaussian distribution but are independent of each other at any time t.

In magnitude and phase representation:

$$a(t) = \|a(t)\|e^{jq(t)}, \tag{2.4}$$

where

$$q(t) = tan^{-1}(\frac{a_Q(t)}{a_I(t)}), \|a(t)\| = \sqrt{a_I(t)^2 + a_Q(t)^2} \tag{2.5}$$

The random variable q follows a uniform distribution in $[0, 2\pi]$ while $\|a(t)\|$ follows the Raleigh distribution.

The flat fading channel can be interpreted as a random complex gain multiplying to the transmitted signal and hence altering the amplitude and phase of the transmitted signal. Also, from Verdu [13], we have a similar expression. For the random complex gain $A_k[i]$,

$$A_k[i] = A_k R[i], \tag{2.6}$$

where i is an integer representing the discrete time index.
The probability density function of R is:

$$f_R(r) = \frac{r}{\sigma^2}e^{-\frac{r^2}{2\sigma^2}} \text{ , which is the Raleigh distribution} \tag{2.7}$$

and the phase of $A_k[i]$ is uniformly distributed in $[0, 2\pi]$. That is , if θ denotes the phase of $R[i]$, the probability density function of θ is $f_\Theta(\theta) = \frac{1}{2\pi}$. It shows that $A_k[i]$ is a random complex gain multiplying to the transmitted baseband signal, which is the effect of flat fading channel.

(b)Frequency-selective fading channel model in Rappaport[14] and Cheng's lecture notes [15]:

Frequency-selective fading channel model could be expressed as the summation of a series of amplitude-attenuated, time-delayed and phase-shifted replicas with flat-fading parameters corrupting each multipath at any time t. The

mathematical formulation of the channel impulse response is as follows. Assume that there are N multipaths at any time t giving

$$h_b(t,\tau) = \sum_{i=0}^{N-1} a_i(t,\tau) e^{j(2\pi f_c \tau_i(t) + \phi_i(t,\tau))} \delta(\tau - \tau_i(t)) \tag{2.8}$$

Graphically,equation 2.8 is shown in Figure 2.1.

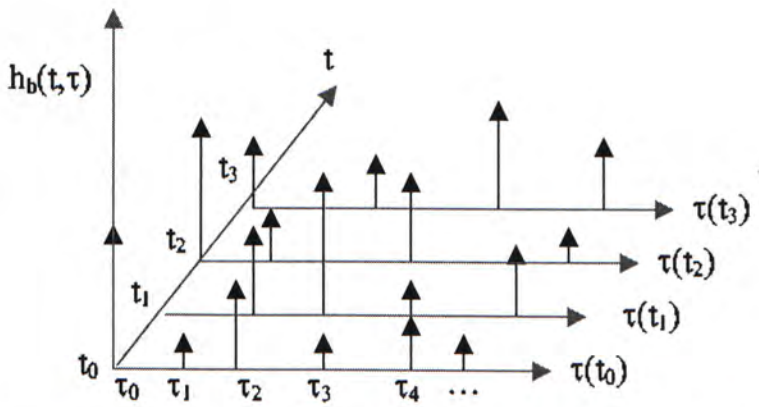

Figure 2.1: An example of the time varying continuous-time impulse response $h_b(t,\tau)$ model of a multipath radio channel

$a_i(t,\tau)$ and $\tau_i(t)$ are the real amplitudes and excess delays of ith multipath component at time t. The phase term $2\pi f_c \tau_i(t) + \phi_i(t,\tau)$ represents the phase shift due to free space propagation of the ith multipath component plus any additional phase shifts encountered in the channel. We choose the frequency-selective fading model in the thesis since we are interested in investigating the inter-symbol interference (ISI) effect caused by correlated multipath signals of the desired user and those of MAI at the base-station receivers.

The *slow* frequency-selective fading model is considered in the thesis by assuming that the channel is time-invariant within the duration of a symbol period. That is, the coherence time is much longer than one symbol period. This is because we are interested in the effect of inter-symbol interference due to the correlated multipaths of the desired user (self-ISI) and those of MAI

at the receivers. Hence, the time-varying effect of the channel parameters is not discussed in our analysis, but it is a critical factor in the investigation of adaptation and tracking ability of a wireless receiver in the fast fading channel in [16].

2.1.3 Combination of K-user CDMA Time Model with the Slow Frequency-Selective Fading Channel Model to form a completed Chip-Synchronous CDMA Time Model

There are some equations modelling the K-user CDMA channel model with the corrupting sources from both dispersive channel mentioned in the section 2.1.2 and additive noise.

Example 1:

From the work of Mudulodu & Paulraj [17],

$$y_m^{(j)}(t) = \sum_{n=-\infty}^{\infty} x^{(j)}(n) h_m^{(j)}(t - nT_c) + v_m^{(j)}(t) \tag{2.9}$$

where,

$h_m^{(j)}$ is the channel response from the transmitter to the mth antenna of the jth user;

$x^{(j)}$ is the transmitted baseband signal of jth user;

$v_m^{(j)}$ is the additive noise;

$1/T_c$ is the signature chip rate;and

n denotes the chip index.

This equation models the received baseband signal $y_m^{(j)}(t)$ of the jth user at mth element in the antenna array. If we sum up all the transmitted signal of the multiple access users within the cell, the following equation will result.

Example 2:

From Ramos,Zoltowski and Liu [18], if we have J users with each of which has

L_k multipaths arriving at the antenna, the received baseband signal could be characterized as:

$$x(t) = \sum_{k=1}^{J} \sigma_k \sum_{l=1}^{L_k} \rho_k^l a(\theta_k^l) s_k(t - \tau_k^l) + n(t) \tag{2.10}$$

and $s_k(t) = \sum_{n=-\infty}^{\infty} b_k(n) c_k^{(n)}(t - nT_b)$

where,

$s_k(t)$ is the baseband signal transmitted from the kth user;

$b_k(n)$ denotes the nth symbol bit value;

$c_k(t)$ represents the code assigned to kth user;

$a(\theta_k^l)$ is the array manifold;

θ_k^l 2-D (azimuth and elevation) is the direction of arrival;

T_b is the bit period;

σ_k characterizes the received amplitude of kth user's direct path;

ρ_k^l represents the complex number showing the attenuated amplitude and shifted phase of kth user's lth multipath;

τ_k^l is the arrival delay of the kth user's lth multipath; and

$n(t)$ denotes the additive white Gaussian noise.

From equation 2.10, this sums each user's self-ISI to give us DS-CDMA communication channel. Similarly, we could add all multiple access users's multipath signals together within the system in equation 2.9 to give

$$y_m(t) = \sum_{allj} y_m^{(j)}(t) \tag{2.11}$$

All the above-mentioned examples show that if we combine the multipath fading channel model in section 2.1.2 with the K-user CDMA channel model in section 2.1.1, this will be the summation of all self-ISI (due to the desired user's own multipaths) and MAI's multipaths with each of them multiplied by a random complex gain which changes the multipath signal's amplitude and phase. Also, there is an arrival delay for each multipath signal.

2.1.4 Spatial Channel Model with Antenna Array [9]

The aforementioned models are the completed chip-synchronous DS-CDMA time models. Since we have an array of antenna elements, we have to derive a suitable model manipulating both temporal and spatial raw received baseband data at each antenna element.

Spatial channel model with antenna array refers to digital beamforming. Digital beamforming combines the two major advances in monolithic microwave integrated circuit (MMIC) technology and digital signal processing (DSP) technology. Beamforming means the spatial filtering operation performed by antenna arrays. If we have an array of antenna elements, we could apply some weighting factors (beamforming weights) by means of digital signal processing technology to modify the received baseband signal's amplitude and phase so that we could sum up our desired user's signals constructively and at the same time we suppress or do not receive those signals suspected to be radiated from the interfering sources. Beam pattern means the spatial response of the beamformer. This will place a null to the spatial direction at which the interfering signal coming to the receiver and point a directive beam towards our desired user's location. Beamformer uses a weighting vector applied across the antenna elements' steering array to form a beam pattern. The following figure shows the details.

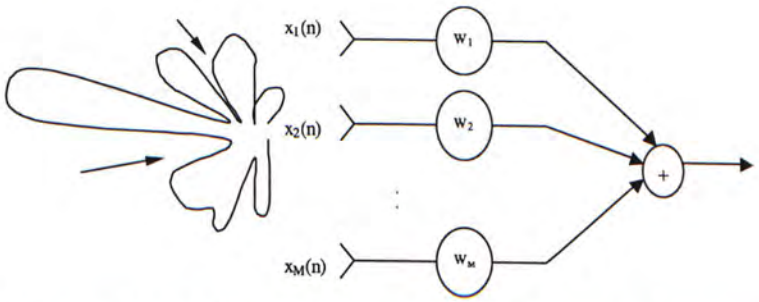

Figure 2.2: An example of the spatial response of an array of antenna elements, known as beampattern, emphasizing signals from desired user's direction of arrival (DOA)

From figure 2.2, at each antenna element, we will receive a raw baseband data. Then the baseband data at each antenna element will be weighted by beamforming weight to give us improved SINR data output by modifying the signals' amplitude and phase and adding them constructively. The purpose of using digital beamforming is to provide different beam patterns for spatial diversity to increase the channel capacity in a cell. There are some common figurations of antenna arrays such as linear, circular and planar arrays. We focus here on the linear antenna array for its simplicity. Also, the performance of a class of blind space-time RAKE receivers we interested does not depend on the antenna array's manifold.

Figure 2.3 shows a uniformly spaced linear array and typical parameters. Equations in the model of the linear array's radiation pattern will also be discussed.

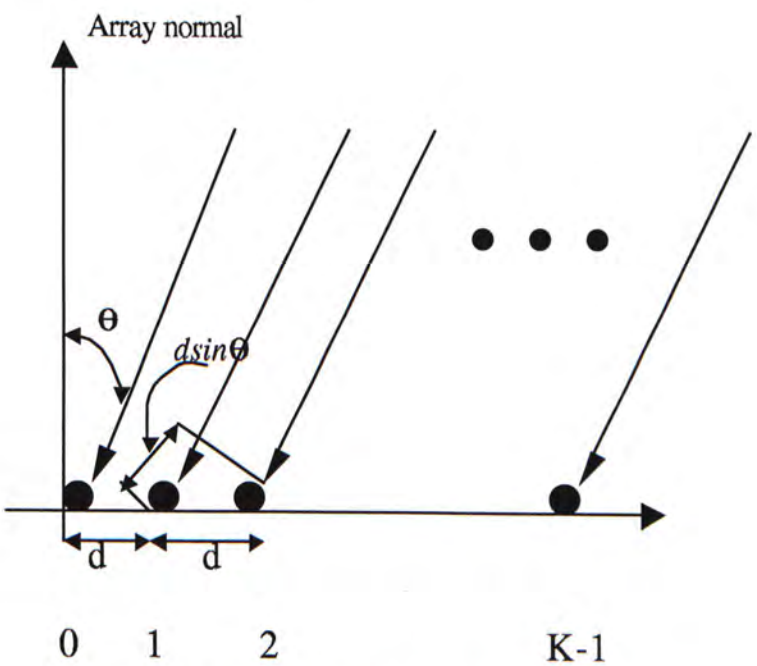

Figure 2.3: A uniformly spaced linear array

The elevation angle of arrival θ is shown in figure 2.3. It is measured from the normal to the direction of impinging plane wave. There are K identical isotropic elements in an antenna array and each element will be weighted by

the beamforming complex weight V_k with $k = 0, 1, \ldots, K-1$. The spacing between each element is d and hence the differential distance between two ray paths is $dsin\theta$ as shown in the figure. If we set the phase of the received signal at the origin to zero, the phase lead of the signal at the kth element relative to element at the origin will be $\kappa kdsin\theta$, where $\kappa = \frac{2\pi}{\lambda}$ and λ = wavelength. Using all the parameters of all the elements, the array factor $F(\theta)$ is expressed as:

$$\begin{aligned} F(\theta) &= V_0 + V_1 e^{j\kappa dsin\theta} + V_2 e^{2\kappa dsin\theta} + \cdots + V_{K-1} e^{j(K-1)\kappa dsin\theta} \\ &= \sum_{k=0}^{K-1} V_k e^{jk\kappa dsin\theta} \end{aligned} \tag{2.12}$$

or in matrix notation,

$$F(\theta) = \mathbf{V^T v} \tag{2.13}$$

where,

$$\mathbf{V} = [V_0, V_1, \cdots, V_{K-1}]^T \tag{2.14}$$

denotes the weighting factor.

The array propagation or array steering vector is $\mathbf{v}$, which contains the angle of arrival information as shown below.

$\mathbf{v} = \left[1, e^{j\kappa dsin\theta}, \cdots, e^{j(K-1)\kappa dsin\theta}\right]^T$

If the complex weight is expressed as:

$$V_k = A_k e^{jk\alpha} \tag{2.15}$$

$F(\theta)$ can be further simplified as:

$$F(\theta) = \sum_{k=0}^{K-1} A_k e^{j(\kappa dsin\theta + k\alpha)} \tag{2.16}$$

From equation 2.16, we could form a directive beam towards a specific angle θ_0 by setting the value α in the complex weight V_k to $-\kappa d sin\theta_0$ in equation 2.15. This is because when the variable θ changes, the magnitude of $F(\theta)$ will be maximum if $\theta = \theta_0$ by setting $\alpha = -\kappa d sin\theta_0$. Hence, with the use of antenna array, different kinds of antenna radiation pattern are formed, especially, it can form a high directive gain towards a specific source. It is like a spatial filter forming a strong radiation beam towards the desired user while nulling out the dominant multiple access interference simultaneously.

Below is an example of using eight linear half-wavelength-spaced antenna array to form a beam pattern pointing towards the desired user's incident beam of zero-degree evaluation angle.

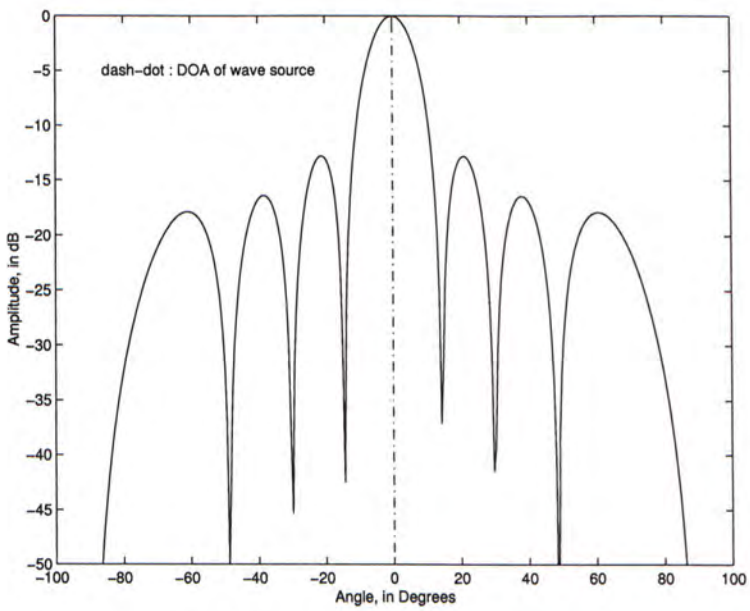

Figure 2.4: An example of the beam pattern of using a half-wavelength-spaced eight-element linear array to produce high directive gain towards direction of arrival (DOA) of the wave source

2.1.5 Joint Space-Time Channel Model in Chip-Synchronous CDMA

The signal model developed in the section 2.1.3 is mostly concerned with the received baseband signal model for CDMA with one antenna element only. In this section, the use of multiple antennas and the detailed space-time model for chip-synchronous CDMA are introduced. The following equations show the details of the *space-time* chip-synchronous CDMA model.

Example 1:

In the paper of Chen et.al.[1], the discrete-time raw baseband data $\mathbf{x}(t)$ is shown below:

$$\begin{aligned}\mathbf{x}(t) = &\sum_{k=1}^{P} \rho_k \sum_{m=0}^{N_b-1} \mathbf{a}(\theta_k^d)\mathbf{D}(m)c(t - mT_b - \tau_k) \\ &+ \sum_{i=1}^{J} \sum_{m=0}^{N_b-1} \mathbf{a}(\theta_i)\sigma_i \mathbf{D}_i(m)c_i(t - mT_b) + \mathbf{n}_w(t)\end{aligned} \tag{2.17}$$

$\mathbf{x}(t)$ represents the $M \times 1$ snapshot column vector containing the outputs of each of the M antennas comprising the array at time t. $\mathbf{a}(\theta)$ is the spatial response of the array, where θ is the direction of arrival (DOA) of a given source. There is no model assumed for θ and the above model works for any array geometry. The other notations are as follows. $1/T_b$ is the symbol rate common to all sources. P represents the number of different paths from which the signal of interest (SOI) arrives. θ_k^d is the directions associated with the k th path. τ_k is the corresponding relative delay of the kth path. ρ_k is the complex amplitude of the kth multipath arrival for the SOI at the reference element. $D(m)$ and $D_i(m)$ are the digital information sequences for the SOI and MAI sources, respectively. J broadband interferers (MAI) impinge on the array. σ_i is the complex amplitude of the ith interferer at the reference element of the array. $c(t)$ and $c_i(t)$ are the spreading waveforms for the SOI and ith MAI, respectively. The vector $\mathbf{n}_\omega(t)$ contains white noise. N_b is the number of bits

over which all parameters characterizing the model in 2.17 are assumed to be constant. The spreading waveform $c_i(t)$ for the ith MAI is modeled as

$$c_i(t) = \sum_{l=0}^{N_c-1} s_i(l) p_c(t - lT_c - T_{off_i}) \tag{2.18}$$

where,

$(1/T_c)$ is the chip rate;

$s_i(l)$ represents PN sequence;

$p_c(t)$ denotes the chip waveform assumed common to all sources;

N_c is the number of chips per bit common to all MAI;and

T_{off_i} is the timing offset of the $i$thh MAI relative to the desired user.

The ith row element in column vector $\mathbf{x}(t)$ contains the received baseband signal at the ith element in the antenna array of size $M \times 1$ at any time t. Therefore, if the sampling rate is 2 samples per chip and 127-chip signature sequence is used, there will be 254 discrete-time samples in each symbol duration. Assuming an antenna array has 4 elements, at any time t, there will be 4×1 column data vector and hence, there will be 254 column data vectors in each symbol duration.

Example 2:

From the work of Wong et. al. [2], the baseband signal $\mathbf{r}(t)$ received at the base-station is characterized by:

$$\mathbf{r}(t) = \mathbf{y}(t) + \mathbf{n_I}(t) + \mathbf{n_B}(t) + \mathbf{n_W}(t) \tag{2.19}$$

with $\mathbf{y}(t)$ representing the desired user's contribution:

$$\mathbf{y}(t) = \sqrt{2P_1} \sum_{\lambda=1}^{L_1} g_1 a_1(t - T_1 - \tau_{1,\lambda}) e^{j(w_c(T_1)+\tau_{1,\lambda})} \mathbf{d}_{1,\lambda} \tag{2.20}$$

Similar to example 1, $\mathbf{r}(t)$ represents the $D \times 1$ vector at any time t, which represents the received baseband signal at the antenna array of D elements.

$\mathbf{n}_W(t)$ represents AWGN. The MAI contribution $\mathbf{n}_I(t)$ is given by:

$$\mathbf{n}_I(t) = \sum_{k=2}^{K} \sqrt{2P_k} \sum_{\lambda=1}^{L_k} g_{k,\lambda} a_k(t - T_k - \tau_{k,\lambda}) \cdot e^{-j\omega_c(T_k+\tau_{k,\lambda})} \mathbf{d}_{k,\lambda} \qquad (2.21)$$

and the narrowband interference $\mathbf{n}_B(t)$ is denoted as:

$$\mathbf{n}_B(t) = \sum_{k=K+1}^{K+K_B} \sqrt{2P_k} g_k e^{j\delta_k t} \mathbf{d}_k \qquad (2.22)$$

L_k is the number of propagation paths from the kth transmitter to the antenna array. The parameters $\tau_{k,\lambda}$,$g_{k,\lambda}$ and $\mathbf{d}_{k,\lambda}$ represent the delay, the complex gain and the array response vector associated with the λ th path of the signal from the kth transmitter. In equation 2.22, the parameters P_k, g_k , δ_k and $\mathbf{d}_k$ represent the power, the complex gain , the frequency deviation from ω_c, and the array response vector associated with the tone indexed by k for $K + 1 \leq k \leq K + K_B$ respectively. Without loss of generality, we assume that $\delta_k \neq \delta_l$ for $k \neq l$.

Example 3:

In the work of Pados and Batalama [19], the equation modelling the received baseband data at the base-station receiver is $\mathbf{x}(t)$:

$$\mathbf{x}(t) = \sum_{i} \sum_{k=0}^{K-1} b_k(i) \sum_{n=0}^{N-1} c_{k,n} \sqrt{E_k} s_k(t - iT - nT_c - \tau_k) \mathbf{a}_{k,n} + \mathbf{n}(t) \qquad (2.23)$$

where,

$$c_{k,n} = \alpha_{k,n} e^{-j(2\pi f_c(nT_c)+\gamma_k)}$$

$$\mathbf{a}_{k,n}[m] = e^{j2\pi(m-1)(d/\lambda)sin(\theta_{k,n})}, \qquad m = 1, \ldots, M$$

T denotes the information bit duration;

γ_k is the random carrier phase shift;

K represents the total number of multiple access users in the system;and

N is the total number of resolvable multipaths per user.

The $M \times 1$ array response vector $\mathbf{a}_{k,n}$ represents the nth path of the kth user signal. $\theta_{k,n}$ identifies the angle of arrival of the nth multipath signal from the kth user. λ is the carrier wavelength and d which is usually equal to $\lambda/2$ is the element spacing of the antenna. $\mathbf{n}(t)$ denotes an M-dimension complex Gaussian noise process that is assumed white both in time and space. $c_{k,n}$ is the channel coefficient of kth user's nth path. $b_k(i) \in \{-1, 1\}$ is the ith transmitted data bit and E_k denotes energy. The normalized user signature waveform $s_k(t)$ of the kth user is shown below.

$$s_k(t) = \sum_{l=0}^{L-1} d_k[l]\psi(t - lT_c) \tag{2.24}$$

$d_k[l] \in \{-1, 1\}$ denotes the lth bit of the spreading sequence of the kth user. $\psi(t)$ is the chip waveform and T_c is the chip period. In matrix form, we define the data matrix, $\mathbf{X}_{M\times(L+N-1)}$ as:

$$\mathbf{X}_{M\times(L+N-1)} = [\mathbf{x}(0), \mathbf{x}(T_c), \cdots, \mathbf{x}((L+N-1)T_c)] \tag{2.25}$$

where,

M is the total number of elements in an antenna array;

$L = T/T_c$ is the processing gain;and

$(L + N - 1)$ denotes the total number time samples prepared for one-slot detection of ith information symbol.

From the above examples, they show that the *space-time* data models for DS-CDMA channel are to collect the received baseband signal at any time t from all the elements in the antenna array in the form of a snapshot matrix or a snapshot vector for further manipulation.

Moreover, we could consider a number of symbol durations in the received raw baseband discrete-time data for later analysis stage. Then, at each antenna element, we will have a array of discrete-time baseband data which could be collected as a row vector. Therefore, for each antenna element, we will have

one row vector storing all the discrete-time baseband data in a number of symbol durations. If we have four antenna elements, we will have four row vectors putting into one data block matrix, which represents our collected raw baseband discrete-time data for further signal processing stage.

Supposing a 127-chip signature sequence is used, the size of the data block matrix will be 4×254 with an antenna array of 4 elements, assuming that the sampling rate is 2 samples per chip and 1 symbol interval is considered. In the thesis, similar data block matrix is used for manipulating the received raw baseband discrete-time data from all the antenna elements.

2.1.6 Challenges to Blind Space-Time Processing in a base-station CDMA Receiver

When a mobile phone user transmits its information-bearing signal, this signal will become several multipaths arriving at the base-station. These mutlipaths are the amplitude-attenuated, phase-shifted and time-delayed versions of the origianl transmitted signal. If there is a conventional RAKE receiver installed at the base-station, it could resolve and combine the desired user's multipaths constructively with the assumption that the fading channel parameters are priori known.

Space-time processing could be applied to the conventional RAKE receiver if there is an array of antenna elements available at the base-station. This antenna array signal processing provides extended spatial and temporal reception diversity so that the probability of collecting less distorted multipath signal will increase.

There are several key challenges of such a space-time antenna array signal processing.

(a) Fading channel response

In order to constructively sum the desired signal's multipaths, the receiver's

space-time processor needs to know the multipaths' fading parameters such as the arrival angles, arrival delays, distorted amplitudes and phases. However, these fading parameters are typically not a priori known and rapidly time-varying. These fading parameters need to be adaptively estimated, sometimes by using training sequences. The training symbols are the non-information-carrying pilot symbols in the information data stream, or by setting aside a dedicated channel, which consumes precious channel bandwidth. In IS-95 standard, there is a specified channel named as "pilot channel" for sending training sequence between the base-station and the mobile phone users for estimating the fading channel parameters.

There is an advantage if the space-time processor in the wireless receiver can "blindly" sum the desired signal's multipaths and suppress the dominant multiple access interference without consuming the extra channel bandwidth.

(b) Single-user-type detectors in space-time RAKE receivers and near-far problem

There are different kinds of detectors developed such as the linear type and non-linear type in the wireless CDMA multi-user detection. For linear type detectors, there are single-user-type matched filter, minimum mean-square error (MMSE) multi-user detector and the decorrelating detector. The non-linear type is composed of the decision feedback detectors such as successive and parallel interference cancellation detectors in Verdu [13].

The single-user-type detector can be *interpreted* as the "matched filter" used to match the specific *signal waveform* representing a corresponding *symbol* in the digital M-ary modulation in Haykin [20]. That is, each user is assigned to have a signature sequence for identification and the single-user-type detector is used to *match* the specific signature to identify the corresponding user. Therefore, the role of the single-user-type detector is like the matched filter which "matches" the specific signature sequence waveform that represents the corresponding user in the DS-CDMA multi-user communication system.

However, due to the effects of a fading channel, the cross-correlation of the transmitted signals among the users is non-zero. If we use the single-user-type detector for each user to detect their own signature waveform, the irreducible error floor will result with respect to each user due to the assumption that the single-user-type detector treats other user's signature waveform as additive white noise, in an averaging approach.

This will lead to a common problem, called, the "near-far" problem, happening within the cell. The user at the edge of the cell will suffer more power loss when it is received at the base station, compared with the received signal level of the user near the base station. The user near the base station will then dominate the received signal power levels at the base station due to the non-zero cross-correlation among the transmitted signal of the users. Therefore, this decreases the SINR of other users and hence the reception quality of other users will be degraded.

Although there is an irreducible error floor when the single-user-type detector is used, it would be an advantage that the receiver needs to know the desired user's signature sequence as only the priori knowledge but not all other users' signature sequences within the CDMA communication system. The receiver's structure would be simpler and its computational complexity would be lower compared with the conventional high performance decorrelating type receivers in Verdu[13].

2.2 Literature Review of Single-User-Type Detectors used in Blind Space-Time DS-CDMA RAKE Receivers

In the thesis, we wish to investigate a class of signal processing schemes that enhances the SINR at the output of the space-time RAKE receiver. In the

received baseband signal, it is classified into two data groups — one group (heretofore designated by S+I+N) contains much of the desired signal's energy plus energy from the interference and noise that degrade the desired signal, the other group (heretofore designated as I+N) of data containing only the interference and noise but little desired signal energy. By comparing the S+I+N data group with the I+N data group, estimation can be made of the interference and noise corrupting the S+I+N delay segment. Blind element-space-only/delay (or element-space/frequency or beamspace/frequency) beams may be formed to constructively sum the SOI's multipaths while rejecting the dominant interferences.

Within this algorithmic family are a variety of approaches to form the S+I+N and I+N data groups. Suard, Naguib, Xu & Kailath [21] as well as Naguib, Paulraj & Kailath [3] use the despread *spatial* data correlation matrix as the S+I+N data group and the un-despread *spatial* data correlation matrix as the I+N group. Although SOI energy is present in both groups, the signature sequence despreading operation greatly enhances the SINR ratio in the S+I+N group relative to the I+N group. This one-dimensional (i.e., spatial) beamforming approach separates the beamformer's spatial processing from the desreading filters' temporal processing, and is thus incapable to exploit the fading channel's *two-dimensional space-time* structure. Liu & Zoltowski [4] extend [3] and [21] to space-time beamforming by using the despread (*space-time*) *space-delay* [1] data correlation matrix as the S+I+N data group and the un-despread *space-time* data correlation matrix as the I+N group. However, the temporal despreading filter *alternates* the multipaths' arrival delay temporal structure for the S+I+N data group. This means the I+N data group becomes a poor estimate of the interference and noise in the S+I+N group, thereby compromising that scheme's performance.

[1]The output of the signature sequence despreading filter is a discrete-"time" sequence along the arrival "delay" axis. To avoid confusion with time and delay, this thesis labels this axis as the delay axis.Hence,"space-delay" is used.

Wong, Lok, Lehnert & Zoltowski [2] alleviate the above problem by exploiting the following insight: the fading channel's multipath delay spread generally occupies only a small fraction of the information symbol duration in a CDMA system, such as the IS-95 standard. Hence, the CDMA de-spreading filter's output (over each symbol's duration) involves one close cluster of "fingers" or "blips" (each of which corresponding to one temporally resolvable time-delayed multipath of the signal of interest — SOI). The S+I+N data group is formed from the despreading filter outputs during the delay segment in each symbol's period containing this cluster of "fingers", whereas the despreading filters' output in the remaining delay segment are formed into the I+N data group. Chen, Zoltowski, Ramos, Chatterjee, & Roychowdhury [1]present the reduced algorithmic computational complexity of [2] by substituting the space-time beamforming with element-space/frequency beamforming or beamspace/frequency beamforming.

When the fading channel's delay spread cannot be assumed to be much smaller than an information symbol's duration (e.g., at very high information data transmission rate, the above schemes [1, 2, 22] are inapplicable). Luo & Blostein [6] as well as Liu & Geraniotis [5] separately propose despreading the received data against a signature sequence orthogonal to the desired signal's signature sequence. The spatial correlation matrix of the outputs from these orthogonal despreading filters form the I+N data group, whereas the S+I+N data group is formed as in [21]. The main difference between [6] and [5] is the way the orthogonal spreading sequence relates to the desired signal's signature sequence. In [6], -1 is multiplied to alternating chips in desired signal's direct-sequence (DS) code, whereas [5] multiplies the second half of the desired signal's DS chip sequence by -1. Because each multiple-access user would need its own orthogonal sequence, these two schemes double the effective "bandwidth" occupies by each user.

2.2.1 A Common Problem among the Signal Processing Schemes

All the above-mentioned schemes which are used in the maximum-SINR blind space-time processing suffer a common *problem*. There is a significant SOI's energy in the I+N data group. This means that the interference and noise estimation from the I+N group would mistake the desired signal as undesired and to be rejected. With even a trace of SOI's energy in the I+N data group, the beamformer would reject a significant portion of the SOI's energy and may let pass much of the interference and noise. This will lower the output SINR and hence increase the bit error rate.

Chapter 3

Novel "Self-Decorrelation" Technique

3.1 Problem with "Blind" Space-Time RAKE Processing Using Single-User-Type Detectors

In this chapter, the proposed **"self-decorrelation technique"** is introduced to improve the performance of the family of blind space-time RAKE receivers proposed by Chen et.al.[1] with the assumption that the multipath delay spread occupies a small fraction of a symbol duration .

Chen,Zoltowski and Ramos [1, 10, 11, 12, 23] recently proposed a family of "blind" maximum-signal-to-interference-plus-noise (maximum-SINR) space-time RAKE receiver structures (with element-space/delay, element-space/frequency or beamspace/frequency versions) for single-user-type DS-CDMA detectors. The pivotal idea underlying this scheme is that the fading channel's multipath delay spread generally occupies only a small fraction of the information symbol duration in a CDMA system, such as the IS-95 standard. Hence, the CDMA de-spreading filter's output (over each symbol's duration) involves one

close cluster of "fingers" or "blips" (each of which corresponding to one temporally resolvable time-delayed multipath of the signal of interest — SOI). The label "S+I+N" is to apply to the delay segment in each symbol's period containing this cluster of "blips" that includes energy from the SOI and the interference and the noise. The remaining delay segment (to be labeled "I+N") contains mostly interference and noise, but also *a trace of SOI energy* due to the SOI's non-zero-lag auto-correlation having non-zero values. By comparing the S+I+N delay segment with the I+N delay segment, estimation can be made of the interference and noise corrupting the S+I+N delay segment. Blind element-space/delay(or element-space/frequency or beamspace/frequency) beams may be formed to constructively sum the SOI's multipaths while rejecting the strong interferences.

The success of the above algorithmic family, however, depends on how "closely" the I+N segment approximates the interference and noise in the S+I+N segment. If the I+N delay segment contains significant SOI energy or even a trace of SOI energy, the resulting beamformer may reject a significant portion of the SOI's energy and may pass much interference and noise.

This thesis suggests a "self-decorrelating" technique that can significantly improve the above blind space-time processors' detection performance, by excising *all residual SOI energy from the I+N delay segment.* This means better estimates of the S+I+N segment's multiuser interference and noise from the I+N delay segment, resulting in more accurate beamforming weights.

This proposed "self-decorrelating" technique works as follows. Suppose the wireless communication channel knows a prior that the maximum delay spread is D chips. We form a set of $DM_c + 1$ vectors corresponding to the SOI's signature sequence shifted by 0 to D chips, where M_c symbolizes the number of time samples per chip duration. Then, we project the data onto the null space of these $DM_c + 1$ vectors to remove all SOI energy. When these data is then despreaded to give a SOI-free estimate of the interference plus

noise situation, the SOI cannot have arrival delay longer than D chips so it suffices to form only these $DM_c + 1$ vectors.

3.2 Review of Zoltowski & Ramos[10, 11, 12] Maximum-SINR Single-User-Type CDMA Blind RAKE Receiver Schemes

3.2.1 Space-Time Data Model

Let the kth user have the N_C-chip signature spreading sequence $\{d_k(c),\ c = 1, \ldots, N_c\}$ and the temporal waveform $c_k(t) = \sum_{c=0}^{N_c} d_k(c)p_c(t - cT_c)$, where T_c denotes the chip duration and $p_c(t)$ represents the chip shape common to all users. Let the receiver have L antennas with possibly uncalibrated and unknown array manifold $\mathbf{a}(\theta)$. Suppose the kth transmitted signal arrives at the receiver as M_k time-delayed multipaths, with the m_kth multipath arriving with a $\tau_{m_k}^{(k)}$ time delay, a $\gamma_{m_k}^{(k)}$ carrier phase, and power $P_{m_k}^{(k)}$ from a direction of arrival and a polarization state defined by the vector $\theta_{m_k}^{(k)}$. Then, the $L \times 1$ baseband measurement at time t equals:

$$\begin{aligned}\mathbf{x}(t) = \ & \sum_{k=1}^{K} \sum_{m_k=1}^{M_k} \sqrt{P_{m_k}^{(k)}}\mathbf{a}(\theta_{m_k}^{(k)}) \sum_{i=0}^{I} \{b_i^{(k)} u(t - iT_b - \tau_{m_k}^{(k)}) \\ & c_k(t - iT_b - \tau_{m_k}^{(k)}) e^{j\gamma_{m_k}^{(k)}}\} + \mathbf{n}(t) \end{aligned} \tag{3.1}$$

where T_b symbolizes the information symbol duration, $u(t)$ denotes a rectangular pulse with unit amplitude for $0 \leq t \leq T_b$ and zero elsewhere, and $\mathbf{n}(t)$ refers to an $L \times 1$ additive noise vector.

This received signal is time-sampled at each antenna at the sampling rate $f_s = M_c/T_c$, where M_c is the number of samples per chip duration and is assumed to be an integer for mathematical simplicity, the sampled output at each antenna is then passed through a de-spreading filter with impulse response

$h(.)$ matched to the kth user's signature spreading sequence. Denoting $r^{(j,k)}(\tau)$ as the cross-correlation between the jth and the kth signature sequences, the kth user's de-spreading filters produce the following $L \times 1$ vector at the L antennas:

$$\begin{aligned}\mathbf{y}_i(\tau) = & \sum_{m_k=1}^{M_k} \sqrt{P_{m_k}^{(k)}} e^{j\gamma_{m_k}^{(k)}} \mathbf{a}(\theta_{m_k}^{(k)}) \{b_i^{(k)} r^{(k,k)}(\tau - \tau_{m_k}^{(k)})\} \\ & + \sum_{j \neq k} \sum_{m_j=1}^{M_j} \sqrt{P_{m_j}^{(j)}} e^{j\gamma_{m_j}^{(j)}} \mathbf{a}(\theta_{m_j}^{(j)}) b_i^{(j)} r^{(j,k)}(\tau - \tau_{m_j}^{(j)})\} + \mathbf{n}(\tau) \quad (3.2)\end{aligned}$$

3.2.2 The Blind Element-Space-Only (ESO) RAKE Receiver with Self-Decorrelation Pre-processing Applied

Assume the communication channel's multipath delay spread DT_c to be much smaller than T_b (as is the case in CDMA standards such as the IS-95), then there exists at most DM_c temporally resolvable "blips" at each information symbol duration at the de-spreading filter's output. Further define $\tau_i^{(S+I+N)} \stackrel{\text{def}}{=} \{\tau : iT_b < \tau \leq iT_b + DM_cT_s\}$ and $\tau_i^{(I+N)} \stackrel{\text{def}}{=} \{\tau : iT_b + DM_cT_s < \tau \leq (i+1)T_b\}$. Let $N_s = M_cN_c$ denote the total number of time samples for a symbol. At the ith information symbol, form the $L \times DM_c$ matrix $\mathbf{Y}_i^{(S+I+N)}$:

$$\mathbf{Y}_i^{(S+I+N)} \stackrel{\text{def}}{=} [\mathbf{y}(iT_b + T_s), \cdots, \mathbf{y}(iT_b + DM_cT_s)]$$

and the $L \times (N_s - DM_c)$ matrix $\mathbf{Y}_i^{(I+N)}$:

$$\mathbf{Y}_i^{(I+N)} \stackrel{\text{def}}{=} [\mathbf{y}(iT_b + DM_cT_s + 1), \cdots, \mathbf{y}(iT_b + N_sT_s)]$$

Then form the two matrices,

$$\widehat{\mathbf{K}}_i^{(S+I+N,ESO)} \stackrel{\text{def}}{=} \mathbf{Y}_i^{(S+I+N)} (\mathbf{Y}_i^{(S+I+N)})^H \quad (3.3)$$

$$\widehat{\mathbf{K}}_i^{(I+N,ESO)} \stackrel{\text{def}}{=} \mathbf{Y}_i^{(I+N)} (\mathbf{Y}_i^{(I+N)})^H, for 1 \leq i \leq I \quad (3.4)$$

The element-space-only beamforming weight vector $\mathbf{w}_i^{(ESO)}$ aims to maximize the SINR:

$$\begin{aligned} SINR &= \frac{\mathbf{w}^H\{\widehat{\mathbf{K}}_i^{(S+I+N,ESO)} - \widehat{\mathbf{K}}_i^{(I+N,ESO)}\}\mathbf{w}}{\mathbf{w}^H\widehat{\mathbf{K}}_i^{(I+N,ESO)}\mathbf{w}} \\ &= \frac{\mathbf{w}^H\widehat{\mathbf{K}}_i^{(S+I+N,ESO)}\mathbf{w}}{\mathbf{w}^H\widehat{\mathbf{K}}_i^{(I+N,ESO)}\mathbf{w}} - 1 \end{aligned}$$

That is, the optimum weight vector is obtained as:

$$\mathbf{w}_i^{(ESO)} \stackrel{\text{def}}{=} \arg\max_{\mathbf{w}} \frac{\mathbf{w}^H\widehat{\mathbf{K}}_i^{(S+I+N,ESO)}\mathbf{w}}{\mathbf{w}^H\widehat{\mathbf{K}}_i^{(I+N,ESO)}\mathbf{w}} \tag{3.5}$$

$\mathbf{w}_i^{(ESO)}$ is derived as the generalized eigenvector corresponding to the largest (in absolute value) generalized eigenvalue of the matrix pencil pair $\{\widehat{\mathbf{K}}_i^{(S+I+N,ESO)}, \widehat{\mathbf{K}}_i^{(I+N,ESO)}\}$. This element-space-only (ESO) beamformer [1, 10, 11, 12, 23] implements a RAKE receiver with separable spatial processing and temporal processing, which is one of the versions among the family of blind space-time RAKE receivers in Chen et.al.[1] and Zoltowski et.al.[10, 11, 12].

Assume a binary symbol constellation, define the $L \times N_s$ data matrix at the ith symbol as:

$$\begin{aligned} \mathbf{X}(i) &= [\mathbf{x}(iN_s), \mathbf{x}(iN_s+1), \cdots, \mathbf{x}(iN_s+N_s-1)] \\ &= \sum_{k=1}^{K} \underbrace{\left(\mathbf{A}_k\mathbf{\Gamma}_k\mathbf{C}_k b_i^{(k)} + \mathbf{A}_k\mathbf{\Gamma}_k\overline{\mathbf{C}}_k b_{i-1}^{(k)}\right)}_{\stackrel{\text{def}}{=}\mathbf{X}_k(i)} + \mathbf{N}(i) \end{aligned}$$

where,

$$\begin{aligned} \mathbf{A}_k &= \left[\mathbf{a}(\theta_1^{(k)}), \mathbf{a}(\theta_2^{(k)}), \cdots, \mathbf{a}(\theta_{M_k}^{(k)})\right] \\ \mathbf{\Gamma}_k &= \text{diag}(\sqrt{P_1^{(k)}}, \sqrt{P_2^{(k)}}, \cdots, \sqrt{P_{M_k}^{(k)}}) \\ \mathbf{C}_k &= \left[\mathbf{c}_k(\tau_1^{(k)}/N_s); \mathbf{c}_k(\tau_2^{(k)}/N_s); \cdots; \mathbf{c}_k(\tau_{M_k}^{(k)}/N_s)\right] \\ \overline{\mathbf{C}}_k &= \left[\overline{\mathbf{c}}_k(\tau_1^{(k)}/N_s); \overline{\mathbf{c}}_k(\tau_2^{(k)}/N_s); \cdots; \overline{\mathbf{c}}_k(\tau_{M_k}^{(k)}/N_s)\right] \\ \mathbf{N}(i) &= [\mathbf{n}(iN_s), \mathbf{n}(iN_s+1), \cdots, \mathbf{n}(iN_s+N_s-1)] \end{aligned}$$

where *diag* denotes a diagonal matrix having the parameters $\{\sqrt{P_i^{(k)}},\ i = 1, \cdots, M_k\}$ as its diagonal elements.

Furthermore, for $m = 1, \cdots, DM_c$:

$$\mathbf{c}_k(m) = \left[\underbrace{0, \cdots, 0}_{m-1}, c_k(1), c_k(2), \cdots, c_k(N_s - m + 1)\right] \tag{3.6}$$

$$\overline{\mathbf{c}}_k(m) = \left[c_k(N_s - m + 2), c_k(N_s - m + 3), \cdots, c_k(N_s), \underbrace{0, \cdots, 0}_{N_s - m + 1}\right] \tag{3.7}$$

Note that $c_k(n) = c_k(nT_c/M_c)$. and $\overline{\mathbf{c}}_k(1) = \underbrace{[0, \cdots, 0]}_{N_s}$. The lth row of the matrix $\mathbf{X}_k(i)$ must lie in row span of the $(2DM_c - 1) \times N_s$ matrix

$$\mathbf{S}_k \stackrel{\text{def}}{=} [\mathbf{c}_k(1); \mathbf{c}_k(2); \cdots; \mathbf{c}_k(N); \overline{\mathbf{c}}_k(2); \overline{\mathbf{c}}_k(3); \cdots; \overline{\mathbf{c}}_k(N)] \tag{3.8}$$

The row span of $\mathbf{S}_k$ is the same as the subspace spanned by the kth user's spreading sequence delayed up to DM_c time samples. There exist $2DM_c - 1$, instead of DM_c vectors because consecutive symbols in the kth user's data sequence may differ in value.

Define the **"self-decorrelating" orthonormal projector** for the kth user as

$$\mathbf{P}_k^{\perp} \stackrel{\text{def}}{=} \mathbf{I} - \underbrace{\mathbf{S}_k^T(\mathbf{S}_k\mathbf{S}_k^T)^{-1}\mathbf{S}_k}_{\stackrel{\text{def}}{=}\mathbf{P}_k} \tag{3.9}$$

Projecting the time-sampled signal received at each antenna through this self-decorrelating projector $\mathbf{P}_k^{\perp}$,

$$\begin{aligned}\widetilde{\mathbf{X}}(i) &= \mathbf{X}(i)\mathbf{P}_k^{\perp} \\ &= \left\{\sum_{j \neq k}(\mathbf{A}_j\mathbf{\Gamma}_j\mathbf{C}_j b_i^{(j)} + \mathbf{A}_j\mathbf{\Gamma}_j\overline{\mathbf{C}}_j b_{i-1}^{(j)}) + \mathbf{N}(i)\right\}\mathbf{P}_k^{\perp}\end{aligned}$$

because $\mathbf{X}_k(i)\mathbf{P}_k^{\perp} = 0$. Note that $\widetilde{\mathbf{X}}(i)$ no longer contains any SOI energy. $\widetilde{\mathbf{X}}(i)$, in the proposed scheme, is to substitute $\{\mathbf{Y}_i^{(I+N)}\}$ to form the I+N correlation matrix $\widehat{\mathbf{K}}_i^{(I+N,ESO)}$. That is, the signature sequence de-spreading process

is no longer necessary to obtain $\widehat{\mathbf{K}}_i^{(I+N,ESO)}$. On the other hand, $\widehat{\mathbf{K}}_i^{(S+I+N,ESO)}$ is to remain as defined in the original algorithm [1, 10, 11, 12, 23].

3.3 Physical Meaning of Self-Decorrelation Pre-processing

If the "self-decorrelator" is examined in mathematical aspect, this is an orthogonal projector used to extract the interference and noise components, which is equivalent to reject all possible SOI's multipaths in the received raw baseband discrete-time data. These interference and noise components will subsequently be used to formulate I+N spatial correlation matrix which is then used to perform generalized eigen-decomposition with S+I+N spatial correlation matrix to derive the beamforming weight vector $\mathbf{w}$. The role of the self-decorrelator is to remove all SOI's multipaths. The well-approximated or less-distorted interference and noise components are obtained after passing the raw baseband data through the self-decorrelator because the SOI's multipaths are correlated with the mulitple access interfering sources' multipaths in constantly changing channel environment. Hence, clean interference-plus-noise components from the raw baseband data could not be obtained. Similarly, a pure SOI's contribution could not be extracted by passing the raw baseband data through the SOI's matched filter. This class of family of receivers, however, uses the estimated contribution of SOI and the estimated contribution of MAI and noise in raw baseband data implicitly by forming S+I+N spatial correlation matrix and I+N spatial correlation matrix respectively. These two matrices will then be used to derive the beamforming weight $\mathbf{w}$ from the generalized eigen-decomposition of this matrix pencil pair. So, the algorithms used in this class of receivers do not explicitly obtain the exact interference-plus-noise components and the SOI component contributing to the raw baseband data, but

extract the well-approximated components of SOI and interference-plus-noise for deriving the beamforming weight vector by forming two spatial correlation matrices.

The "self-decorrelator" could be interpreted in linear filtering point of view. Matrix $\mathbf{S}_k$ in equation 3.8 contains the time-sampled SOI's signature waveform and its time-delayed versions up to the maximum possible delay spread. The analogy of this formulation might be the linear filtering by convolution operation. If a signal $x(t)$ is passed through the linear filter with impulse response $h(t)$, the convolution operation gives the output signal $y(t)$ by:

$$y(t) = \int_{-\infty}^{+\infty} x(t-\tau)h(\tau)d\tau \tag{3.10}$$

where t denotes the continuous time index

The output signal value $y(t)$ at any time t, from the mathematical point of view, is the continuous-variable inner product between impulse response $h(\tau)$ and the time-shifted versions of input signal $x(t-\tau)$ over the region $\tau \in \{-\infty, +\infty\}$. A specified signal component in the input signal $x(t)$ is obtained by defining the impulse response $h(t)$. So, the inner product operation at any discrete-time instant between the baseband data matrix $\mathbf{X}(i)$ and the matrix $\mathbf{P}_k(= \mathbf{I} - \mathbf{P}_k^{\perp})$ is to let all possible SOI's multipaths pass through the filter $\mathbf{P}_k$ because the filter $\mathbf{P}_k(= \mathbf{S}_k^T(\mathbf{S}_k\mathbf{S}_k^T)^{-1}\mathbf{S}_k)$ is formed by collecting various time-delayed versions of SOI's signature waveform in matrix $\mathbf{S}_k$ of equation 3.8. Hence, the approximated SOI contribution is obtained. In contrast, if the matrix $\mathbf{P}_k^{\perp}(= \mathbf{I} - \mathbf{P}_k)$ is used as the filter, the SOI-free interference-plus-noise components are well estimated.

The time-delayed signature waveforms $\bar{\mathbf{c}}_k(2), \bar{\mathbf{c}}_k(3), \ldots, \bar{\mathbf{c}}_k(N)$ in matrix $\mathbf{S}_k$ of equation 3.8 are not reductant because we need to consider all possible SOI's multipaths arriving at the ith symbol duration. So, we need to include all possible SOI's multipaths which originally belong to the $(i-1)$th symbol

duration but have its tails extending to the ith symbol interval. The time-sampled signature waveform transmitted in the $(i-1)$ symbol duration might have a different sign (if BPSK is used) compared with those time-delayed signature waveforms in ith symbol interval; otherwise, those extended time-delayed multipath versions in the previous symbol duration could be ignored since $\bar{\mathbf{c}_k}(2), \bar{\mathbf{c}_k}(3), \ldots, \bar{\mathbf{c}_k}(N)$ could be expressed as the linear combination of the time-delayed versions $\mathbf{c}_k(0), \mathbf{c}_k(1), \ldots, \mathbf{c}_k(N)$.

The equation 3.9 formulating the self-decorrelator could be analogized as the following derivation of extracting the noise component from the input random signal $x(t)$ using Wiener filtering. Suppose a continuous-time input signal $x(t)(= s(t)+n(t))$ is passed through a Wiener filter and the approximated signal component $\hat{s}(t)$ is the desired output signal.

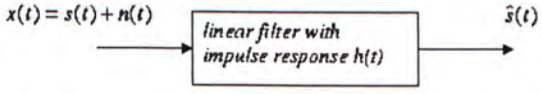

Figure 3.1: Approximated signal component $\hat{s}(t)$ as an output

The transfer function $H(\omega)$ corresponding to the impulse response $h(t)$ is:

$$H(\omega) = \frac{G_{ss}(\omega)}{G_{ss}(\omega) + G_{nn}(\omega)} \tag{3.11}$$

$G_{ss}(\omega)$ is the power spectral density of the random signal $s(t)$ and $G_{nn}(\omega)$ is the power spectral density of the additive noise. Variable $\omega(= 2\pi f)$ symbolizes the continuous frequency index. The signal component $s(t)$ in $x(t)$ is assumed to be independent to the noise $n(t)$. So, the approximated noise component $\hat{n}(t)$ is explicitly extracted using the transfer function $H'(\omega)$ which is defined as:

$$H'(\omega) = \frac{G_{nn}(\omega)}{G_{ss}(\omega) + G_{nn}(\omega)} = 1 - H(\omega)$$

The detailed diagram is shown below.

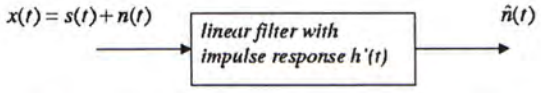

Figure 3.2: Approximated noise component $\hat{n}(t)$ as an output

The derived equation of $H'(\omega)$ (corresponding to the impulse response $h'(t)$) is like the equation of self-decorrelator $P_k^{\perp}$ in equation 3.9. Their roles are to reject the desired signal component in the input data. However, the signal $s(t)$ and the noise $n(t)$ are independent random processes while the multipaths of SOI are correlated with those of MAI in real fading channel environment.

3.4 Simulation Results

Monte Carlo simulations are used to verify the efficiency of the proposed self-decorrelator technique and demonstrate the notable improvements effected for the blind ESO version of the original algorithms in [1, 10, 11, 12, 23]. All simulations below involve a eight-element half-wavelength-spaced linear array. 127-chip Gold codes are used as spreading sequences (with cross-correlation $r^{(j,k)} = r$ among sequences at 0.28, unless otherwise stated) for the BPSK data symbol sequences, which are independent over time and among all the sources. The channel's multipath delay equals 10 chip periods. $\gamma_{m_k}^{(k)}$ is uniformly distributed in $(0, \pi]$ and independent across all multipaths and from trial to trial. A synchronous model with perfect chip synchronization was assumed for the direct path. $M_c = 2$. The SNR figures in all figures are defined with respect to the SOI's direct path's power; and the all SIR figures in all figures are computed with respect to the SOI's and the interference's direct paths. Other details are listed in each figure's caption. Also the hypothetical (and optimum, with respect to beamforming) case where no SOI's energy exists in the I+N segment is also included.

In Fig.3.3, the scenario is as follows. The SOI arrives as a direct path from 0° and a 2-chip delayed path from 10° and $6dB$ weaker than the direct

path. Two multiple-access interference arrive from 40° with a 5-chip delay and from $-20°$ with a 40-chip delay, respectively $20dB$ and $25dB$ stronger than the SOI's direct path. The SNR equals $5dB$.

This figure (Fig.3.3) plots the ESO spatial beam patterns for one particular Monte Carlo experiment, with and without the proposed self-decorrelating pre-processing. Though the interference is well nulled with or without self-decorrrelator pre-processing, the proposed technique produces a beam peak that matches the arrival angles of BOTH paths of the SOI. This is because the non-zero self-correlation of the SOI's signature sequence implies that the SOI's direct path appears in I+N delay segment and is consequentially mistaken as a weak interferer and is nulled. Without the proposed technique the 0° SOI path is significantly attenuated. Note that the self-decorrelator's beam pattern closely approximates the hypothetical case's beam pattern.

Fig.3.4 to Fig.3.6, respectively, show the proposed technique's effects on the SINR of the beamformer output at various SNR, SIR or cross-correlation coefficients (between the SOI and interference signature sequences). Each data point involves 300 independent Monte Carlo experiments, unless stated otherwise.

In Fig.3.4 , the scenario is described as follows. The SOI arrives as a direct path from 0° and a 2-chip delayed path from 3° and $6dB$ weaker than the direct path. One multiple-access interference arrives as two multipaths from 40° and $-20°$ with arrival delays that are independent and uniformly distributed over the entire symbol duration (but always equal to an integral chip period). The second path is always 6dB weaker than the first. The SNR equals $20dB$.

This figure (Fig.3.4) shows a consistent $17dB$ improvement in the beamformer output's SINR at a very wide range of the raw data's SIR. The proposed self-decorrelator pre-processing technique consistently approximates the hypothetical ideal case's SINR, with the beamformer output SINR increasing linearly with the input SNR. This may suggest the removal of the error floor

from the near-far situation present at high SNR's.

In Fig.3.5 , the simulation scenario is as follows. The SOI arrives as a direct path from 0° and a 2-chip delayed path from 10° and $3dB$ weaker than the direct path. One multiple-access interference arrives as two multipaths from 20° and $-10°$ with arrival delays that are independent and uniformly distributed over the entire symbol duration (but always equal to an integral chip period). The second path is always $3dB$ weaker than the first. The SIR equals $-20dB$.

This figure (Fig.3.5) shows that the proposed technique offers $10dB$ to $20dB$ beamformer output SINR improved resistance against the near-far problem for a very low SIR at $-20dB$. This improved robustness against the near-far problem is realized through a beamformer that more precise matches the SOI's and the interference's spatial signatures. For the entire SNR range, the proposed self-decorrelator pre-processing technique again consistently approximates the hypothetical ideal case's SINR.

In Fig.3.6, the scenario is as follows. Same signal and interference scenario as in Figure 3.5, except the SOI's delayed path arrives 10 chip periods late, and the interference's multipath arrival delays are respectively 0 and 10 chip periods. The SNR equals $25dB$.

Fig.3.6 shows the proposed technique's improved robustness against the near-far problem from another perspective than in Fig.3.5. The proposed technique consistently approximates the hypothetical ideal case up to a cross-correlation coefficient of 0.99. The original algorithm in [1, 10, 11, 12, 23] shows notable drop-off in performance from the uncorrelated case beginning at a 0.3 cross-correlation coefficient.

The four graphs described above are shown below.

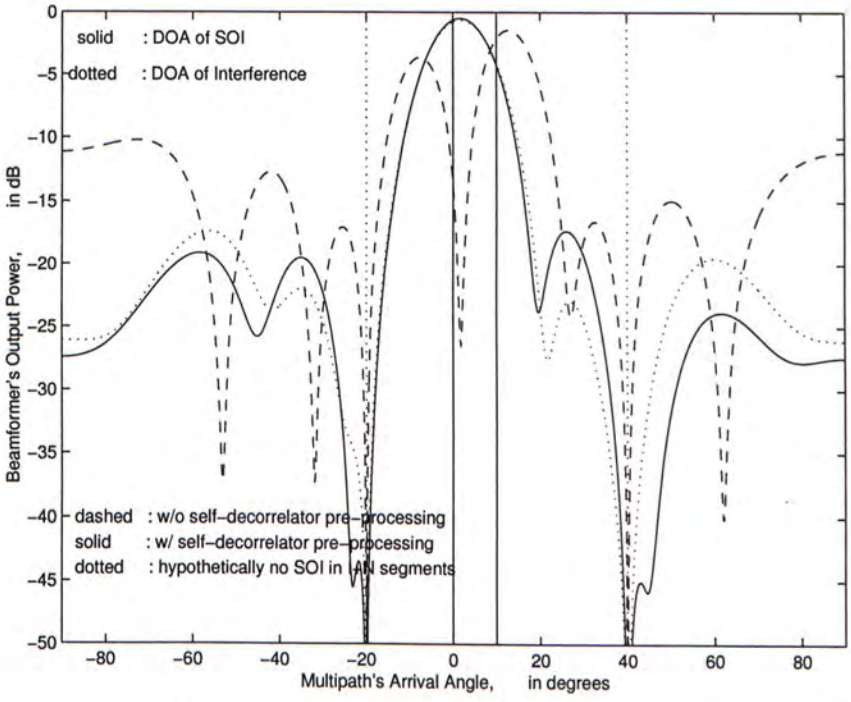

Figure 3.3: ESO beam pattern,with and without the self-decorrelator

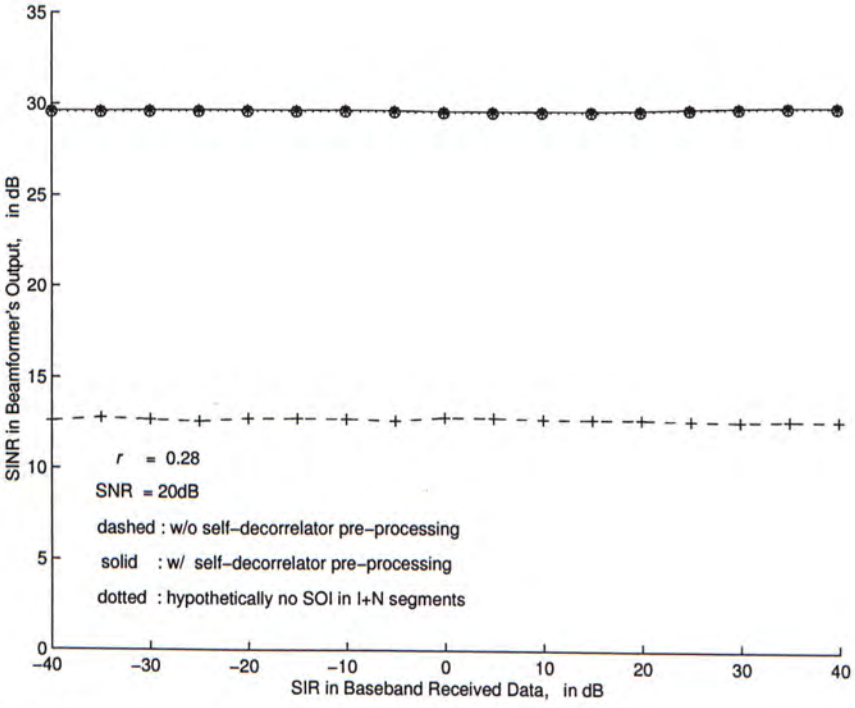

Figure 3.4: The beamformer output's SINR versus the despreading filter input's SIR,with and without the self-decorrelator

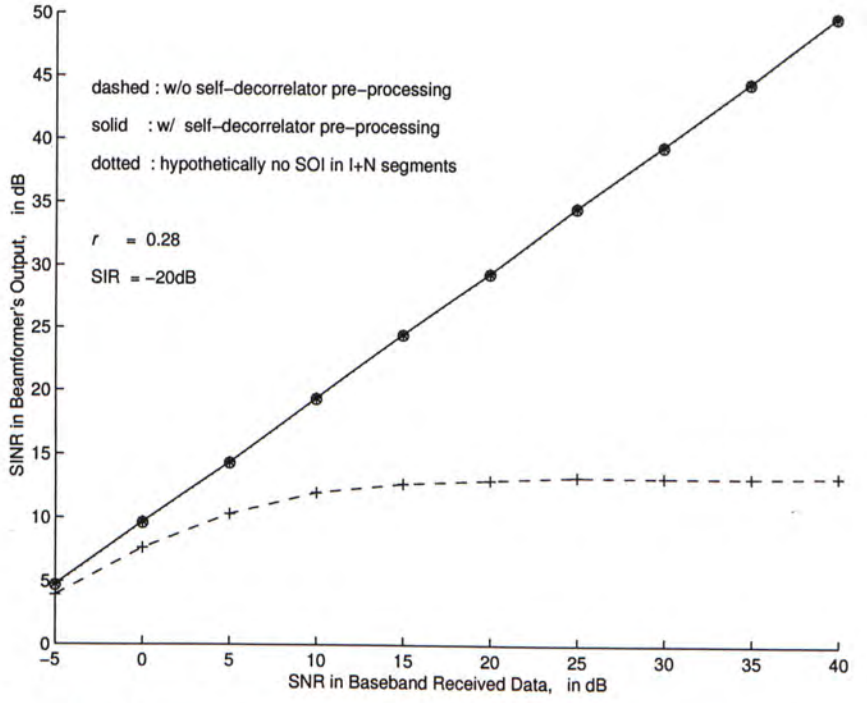

Figure 3.5: The beamformer output's SINR versus the despreading filter input's SNR, with and without the self-decorrelator

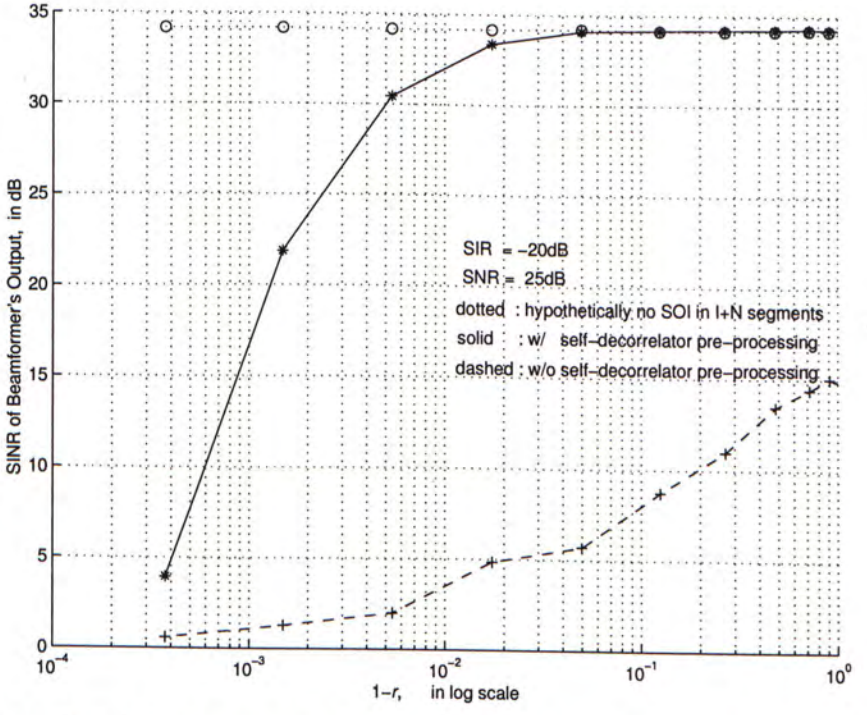

Figure 3.6: The beamformer output's SINR versus the cross-correlation coefficient among spreading sequences, with and without the self-decorrelator

Table 3.1: Summary list of parameter values in figure 3.3

	1^{st} path	2^{nd}path
Angles of arrival of SOI's multipaths	0°	10°
Angles of arrival of MAI's multipaths	40°	
	−20°	
Arrival time delay of SOI's multipaths	0 chip	2 chips
Arrival time delay of MAI's multipaths	5 chips	
	40 chips	
SIR	$-20dB$	
	$-25dB$	
SNR	$5dB$	$6dB$ weaker than $1st$ path

Table 3.2: Summary list of parameter values in figure 3.4

	1^{st} path	2^{nd}path
Angles of arrival of SOI's multipaths	0°	3°
Angles of arrival of MAI's multipaths	40°	−20°
Arrival time delay of SOI's multipaths	0 chip	2 chips
Arrival time delay of MAI's multipaths	random within a	random within a
	symbol interval	symbol interval
SIR	-40 to $40dB$	$6dB$ weaker
		than 1^{st} path
SNR	$20dB$	$6dB$ weaker
		than 1^{st} path

Table 3.3: Summary list of parameter values in figure 3.5

	1^{st} path	2^{nd}path
Angles of arrival of SOI's multipaths	0°	10°
Angles of arrival of MAI's multipaths	20°	−10°
Arrival time delay of SOI's multipaths	0 chip	2 chips
Arrival time delay of MAI's multipaths	random within a symbol interval	random within a symbol interval
SIR	$-20dB$	$3dB$ weaker than $1st$ path
SNR	−5 to $40dB$	$3dB$ weaker than $1st$ path

Table 3.4: Summary list of parameter values in figure 3.6

	1^{st} path	2^{nd}path
Angles of arrival of SOI's multipaths	0°	10°
Angles of arrival of MAI's multipaths	20°	−10°
Arrival time delay of SOI's multipaths	0 chip	10 chips
Arrival time delay of MAI's multipaths	random within 0 to 10 chips	random within 0 to 10 chips
SIR	$-20dB$	$3dB$ weaker than 1^{st}path
SNR	$25dB$	$3dB$ weaker than 1^{st}path

Chapter 4

"Fractional Self-Decorrelation" Pre-processing

In this chapter, a novel **"fractional self-decorrelation" pre-processing** step for "blind" space-time RAKE processing is introduced. This pre-processing mitigates all problems mentioned earlier in Section 2.1.6 and the temporal structure mismatch problem in Liu & Zoltowski [4] mentioned in Section 2.2. Also, it does not assume that the fading channel's delay spread is much smaller than the symbol duration and does not require additional "bandwidth" for each multiple-access user as in Liu & Geraniotis [5] and Luo & Blostein [6].

4.1 The Blind Maximum-SINR RAKE Receivers in Chen et. al.[1] and Wong et. al.[2]

Wong, Lok, Lehnert & Zoltowski [2] alleviate the temporal structure mismatch problem in Liu & Zoltowski [4] mentioned in Section 2.2 by exploiting the following insight: the fading channel's multipath delay spread generally occupies only a small fraction of the information symbol duration in a CDMA system, such as the IS-95 standard. Hence, the CDMA de-spreading filter's output (over each symbol's duration) involves one close cluster of "fingers" or "blips"

(each of which corresponding to one temporally resolvable time-delayed multipath of the signal of interest — SOI). The S+I+N data group is formed from the despreading filter outputs during the delay segment in each symbol's period containing this cluster of "blips", whereas the despreading filters' output in the remaining delay segment are formed into the I+N data group. Chen, Zoltowski, Ramos, Chatterjee, & Roychowdhury [1] present the reduced algorithmic computational complexity of [2] by substituting the space-time beamforming with element-space/frequency beamforming or beamspace/frequency beamforming. Chen & Zoltowski [22] develop an iterative version of [1].

With the above assumption that the communication channel's multipath delay spread DT_c is much smaller than T_b (as is the case in CDMA standards such as the IS-95), then there exists at most DM_c temporally resolvable "blips" at each information symbol duration at the de-spreading filter's output. Further define $\tau_i^{(S+I+N)} \stackrel{\text{def}}{=} \{\tau : iT_b < \tau \leq iT_b + DM_cT_s\}$ and $\tau_i^{(I+N)} \stackrel{\text{def}}{=} \{\tau : iT_b + DM_cT_s < \tau \leq (i+1)T_b\}$. Let $N_s = M_cN_c$ denote the total number of time samples for a symbol. At the ith information symbol, form the $L \times DM_c$ matrix $\mathbf{Y}_i^{(S+I+N)}$:

$$\mathbf{Y}_i^{(S+I+N)} \stackrel{\text{def}}{=} [\mathbf{y}(iT_b + T_s), \cdots, \mathbf{y}(iT_b + DM_cT_s)]$$

and form the $L \times (N_s - DM_c)$ matrix $\mathbf{Y}_i^{(I+N)}$:

$$\mathbf{Y}_i^{(I+N)} \stackrel{\text{def}}{=} [\mathbf{y}(iT_b + DM_cT_s + 1), \cdots, \mathbf{y}(iT_b + N_sT_s)]$$

where L is the number of antenna elements in the antenna array. Then form the two correlation matrices,

$$\widehat{\mathbf{K}}_i^{(S+I+N,ESO)} \stackrel{\text{def}}{=} \mathbf{Y}_i^{(S+I+N)}(\mathbf{Y}_i^{(S+I+N)})^H \tag{4.1}$$

$$\widehat{\mathbf{K}}_i^{(I+N,ESO)} \stackrel{\text{def}}{=} \mathbf{Y}_i^{(I+N)}(\mathbf{Y}_i^{(I+N)})^H, for 1 \leq i \leq I$$

The element-space-only beamforming weight vector $\mathbf{w}_i^{(ESO)}$ aims to maximize

the SINR:

$$SINR = \frac{\mathbf{w}^H\{\widehat{\mathbf{K}}_i^{(S+I+N,ESO)} - \widehat{\mathbf{K}}_i^{(I+N,ESO)}\}\mathbf{w}}{\mathbf{w}^H\widehat{\mathbf{K}}_i^{(I+N,ESO)}\mathbf{w}}$$
$$= \frac{\mathbf{w}^H\widehat{\mathbf{K}}_i^{(S+I+N,ESO)}\mathbf{w}}{\mathbf{w}^H\widehat{\mathbf{K}}_i^{(I+N,ESO)}\mathbf{w}} - 1$$

That is, the optimum weight vector is obtained as:

$$\mathbf{w}_i^{(ESO)} \stackrel{\text{def}}{=} \arg\max_{\mathbf{w}} \frac{\mathbf{w}^H\widehat{\mathbf{K}}_i^{(S+I+N,ESO)}\mathbf{w}}{\mathbf{w}^H\widehat{\mathbf{K}}_i^{(I+N,ESO)}\mathbf{w}} \tag{4.2}$$

$\mathbf{w}_i^{(ESO)}$ is derived as the generalized eigenvector corresponding to the largest (in absolute value) generalized eigenvalue of the matrix pencil pair $\{\widehat{\mathbf{K}}_i^{(S+I+N,ESO)}, \widehat{\mathbf{K}}_i^{(I+N,ESO)}\}$. Though the above Element-Space-Only (ESO) beamformer implements a RAKE receiver with separable spatial processing and temporal processing, other coupled space-time beamforming variations of the above theme are available in [1, 22].

4.2 Fractional Self-Decorrelation Pre-processing

The proposed "fractional self-decorrelation" scheme forms the I+N data group, such that a significantly less amount of SOI energy would remain in the I+N data group compared with [1, 2, 21] and the two methods developed by Liu & Geraniotis [5] and Luo & Blostein [6] mentioned in Section 2.2. This would result in more precise estimation of the interference and noise corrupting S+I+N data group. (No explicit estimation is actually performed for the interference and noise. Instead, a generalized eigen-decomposition procedure will "substract" the interference and noise from the I+N data group from the S+I+N data group to produce a high SINR beamformer's output, hence increased SINR and lower bit error rate.) The S+I+N data group in this proposed scheme would be generated as in Naguib et.al.[3] and Suard et.al.[21] (for spatial beamforming) or Liu et.al.[4] (for space-time beamforming).

The purpose of fractional self-decorrelator, which is not constrained by the assumption of fractional-symbol-duration "fingers", is to form an eigen-subspace which is *orthogonal* to the SOI's subspace generated by choosing a number of largest singular-value column-vectors in the column space formed by the SOI's signature sequence and its time-delayed versions within a symbol period. Towards generating the I+N data group, the pre-despread raw data would first pass through this subspace projector to remove *much of the SOI energy* before despreading with respect to the SOI's signature sequence.

This orthogonal eigen-subspace is formed as follows:

(1) Take the desired signal's N_c-chip spreading sequence and time-delay it to various arrival delays. (If there are M_c discrete-time samples per chip, there would be N_cM_c number of possible delays.)[1]

That is ,

for $m = 1, \cdots, N_cM_c$:

$$\mathbf{c}_k(m) = \left[\underbrace{0, \cdots, 0}_{m-1}, c_k(1), c_k(2), \cdots, c_k(N_cM_c - m + 1)\right]$$

$$\overline{\mathbf{c}}_k(m) = \left[c_k(N_cM_c - m + 2), c_k(N_cM_c - m + 3), \cdots, c_k(N_cM_c), \underbrace{0, \cdots, 0}_{N_cM_c - m + 1}\right]$$

Note that $c_k(n) = c_k(nT_c/M_c)$. and $\overline{\mathbf{c}}_k(1) = [\underbrace{0, \cdots, 0}_{N_cM_c}]$.

(2) use all such cyclically wrapped (i.e., delayed) signature sequences as columns in a matrix $\mathbf{S}$.

$$\mathbf{S}_k \stackrel{\text{def}}{=} \left[\mathbf{c}_k(1)'; \mathbf{c}_k(2)'; \cdots; \mathbf{c}_k(N)'; \overline{\mathbf{c}}_k(2)'; \overline{\mathbf{c}}_k(3)'; \cdots; \overline{\mathbf{c}}_k(N)'\right] \tag{4.3}$$

where $N = N_cM_c$, $\mathbf{c}_k(.)'$ is a column vector.

The column span of $\mathbf{S}_k$ is the same as the subspace spanned by the kth user's spreading sequence delayed up to N_cM_c (total number of data samples

[1]For CDMA systems using long spreading codes with periodicity exceeding one information symbol's duration, the N_c-chip spreading sequence is defined at each symbol as the effective spreading code at that symbol.

within one symbol duration) time samples. There exist $2N_cM_c - 1$, instead of N_cM_c vectors because consecutive symbols in the kth user's data sequence may differ in value.

From now on, the subscript k is dropped for simplified representation.

That is ,

$$\mathbf{S} \stackrel{\text{def}}{=} \left[\mathbf{c}(1)'; \mathbf{c}(2)'; \cdots; \mathbf{c}(N)'; \overline{\mathbf{c}}(2)'; \overline{\mathbf{c}}(3)'; \cdots; \overline{\mathbf{c}}(N)'\right] \tag{4.4}$$

(3) form the $N_cM_c \times N_cM_c$ matrix $\mathbf{SS}^H$, where the superscript H denotes the Hermitian operation.

(4) select the p "largest" eigenvectors (i.e., the eigenvectors corresponding to the p eigenvalues with the largest amplitude) of the matrix $\mathbf{SS}^H$ as the p columns of the $N_cM_c \times p$ matrix $\mathbf{E}^{(p)}$.

(5) form the desired projector $\mathbf{P}^{(p)} \stackrel{\text{def}}{=} \mathbf{I} - \mathbf{E}^{(p)}((\mathbf{E}^{(p)})^H\mathbf{E}^{(p)})^{-1}(\mathbf{E}^{(p)})^H$. This $N_cM_c \times N_cM_c$ projector $\mathbf{P}^{(p)}$ spans would reject much of the SOI energy in the data passing through it. Note that all SOI energy may be blocked by setting $p = N_cM_c$. As $\mathbf{SS}^H$ is generally full rank, picking $p = N_cM_c$ would have produce a full column-rank $\mathbf{E}$ and thus a null-matrix $\mathbf{P}^{(N_cM_c)}$ blocking all interference and noise in addition to the desired signal. Therefore, p should not equal to N_cM_c.

This proposed scheme is labeled "self-decorrelation" because $\mathbf{P}^{(p)}$ removes the SOI energy from the I+N data group using only the SOI's signature sequence. This self-decorrelation concept fundamentally differs from the decorrelation performed in the well-known decorrelating-type multi-user detector. The latter decorrelates various users' respective de-spreading filters' output, whereas the proposed self-decorrelating scheme decorrelates the SOI's S+I+N delay segment from its I+N segment in order to produce a "clean" (i.e., free of SOI energy) I+N correlation matrix for the subsequent SINR maximization eigen-decomposition. Unlike the decorrelating-type detector, the proposed self-decorrelation (1) needs a priori knowledge only of the SOI's signature sequence

but not the other user's signature sequences nor the nominal or effective cross-correlation among all users' signature sequences[2] , and (2) needs to de-spread only for the SOI but not for other multi-user interference (MUI)[3] .

This self-decorrelation scheme is labeled "fractional" because the self-decorrelation is deliberately incomplete – the self-decorrelation projection rejects only the most prominent subspace of the entire vector-space possibly spanned by the SOI's signature sequence and its delayed multipaths. The "fraction" parameter p should be chosen such that as much SOI energy may be blocked without "excessive" distortion of the interference and noise in the resulting I+N data group, such that the information about the interference and noise in the I+N data group represents a good approximation of the interference and noise in the S+I+N data group.

After the fractional self-decorrelator is formed, the raw received baseband data is passed through it to remove the dominant SOI's energy to give a good estimation of interference and noise corrupting to the S+I+N data group. The output from the fractional self-decorrelator is the I+N data group used to form spatial (Naguib et.al.[3]) or space-time (Chen et.al.[1]) correlation matrix for later (maximum SINR)generalized eigen-decomposition to give the optimum element-space-only [4] beamforming weight.

4.3 The Blind Element-Space-Only (ESO) RAKE Receiver with Fractional Self-Decorrelation Pre-processing Applied

Let the kth user have the N_c-chip signature spreading sequence

[2]This is exactly the same a priori information needed by the conventional single-user-type detectors.

[3]That is, only one de-spreading matched-filter is needed.

[4]One of the receiver structures in the family of blind space-time receivers developed in Chen et.al.[1]

$\{d_k(c),\ c = 1, \ldots, N_c\}$ and the temporal waveform $c_k(t) = \sum_{c=0}^{N_c} d_k(c)p_c(t - cT_c)$, where T_c denotes the chip duration and $p_c(t)$ represents the chip shape common to all users. Let the receiver have L antennas with possibly uncalibrated and unknown array manifold $\mathbf{a}(\theta)$. Suppose the kth transmitted signal arrives at the receiver as M_k time-delayed multipaths, with the m_kth multipath arriving with a $\tau_{m_k}^{(k)}$ time delay, a $\gamma_{m_k}^{(k)}$ carrier phase, and power $P_{m_k}^{(k)}$ from a direction of arrival and a polarization state defined by the vector $\theta_{m_k}^{(k)}$. Then, the $L \times 1$ baseband measurement at time t equals:

$$\mathbf{x}(t) = \sum_{k=1}^{K} \sum_{m_k=1}^{M_k} \sqrt{P_{m_k}^{(k)}} \mathbf{a}(\theta_{m_k}^{(k)}) \sum_{i=0}^{I} \{b_i^{(k)} u(t - iT_b - \tau_{m_k}^{(k)}) c_k(t - iT_b - \tau_{m_k}^{(k)}) e^{j\gamma_{m_k}^{(k)}}\} + \mathbf{n}(t)$$

where T_b symbolizes the information symbol duration, $u(t)$ denotes a rectangular pulse with unit amplitude for $0 \leq t \leq T_b$ and zero elsewhere, and $\mathbf{n}(t)$ refers to an $L \times 1$ additive noise vector.

This received signal is time-sampled at each antenna at the sampling rate $f_s = M_c/T_c$, where M_c is the number of samples per chip duration and is assumed to be an integer for mathematical simplicity, the sampled output at each antenna is then passed through a de-spreading filter with impulse response $h(.)$ matched to the kth user's signature spreading sequence. Denoting $r^{(j,k)}(\tau)$ as the cross-correlation between the jth and the kth signature sequences, the kth user's de-spreading filters produce the following $L \times 1$ vector at the L antennas:

$$\mathbf{y}_i(\tau) = \sum_{m_k=1}^{M_k} \sqrt{P_{m_k}^{(k)}} e^{j\gamma_{m_k}^{(k)}} \mathbf{a}(\theta_{m_k}^{(k)}) \{b_i^{(k)} r^{(k,k)}(\tau - \tau_{m_k}^{(k)})\} + \sum_{j \neq k} \sum_{m_j=1}^{M_j} \sqrt{P_{m_j}^{(j)}} e^{j\gamma_{m_j}^{(j)}} \mathbf{a}(\theta_{m_j}^{(j)}) b_i^{(j)} r^{(j,k)}(\tau - \tau_{m_j}^{(j)})\} + \mathbf{n}(\tau)$$

where $N_s = N_c \times M_c$.

Form the $L \times N_s$ matrix $\mathbf{Y}_i^{(S+I+N)}$:

$$\mathbf{Y}_i^{(S+I+N)} \stackrel{\text{def}}{=} [\mathbf{y}(iT_b + T_s), \cdots, \mathbf{y}(iT_b + N_s T_s)]$$

Assume a binary symbol constellation, define the $L \times N_s$ data matrix at the ith symbol as

$$\begin{aligned}\mathbf{X}(i) &= [\mathbf{x}(iN_s), \mathbf{x}(iN_s+1), \cdots, \mathbf{x}(iN_s+N_s-1)] \\ &= \sum_{k=1}^{K} \underbrace{\left(\mathbf{A}_k \mathbf{\Gamma}_k \mathbf{C}_k b_i^{(k)} + \mathbf{A}_k \mathbf{\Gamma}_k \overline{\mathbf{C}}_k b_{i-1}^{(k)}\right)}_{\stackrel{\text{def}}{=} \mathbf{X}_k(i)} + \mathbf{N}(i)\end{aligned}$$

where,

$$\begin{aligned}\mathbf{A}_k &= \left[\mathbf{a}(\theta_1^{(k)}), \mathbf{a}(\theta_2^{(k)}), \cdots, \mathbf{a}(\theta_{M_k}^{(k)})\right] \\ \mathbf{\Gamma}_k &= \text{diag}(\sqrt{P_1^{(k)}}, \sqrt{P_2^{(k)}}, \cdots, \sqrt{P_{M_k}^{(k)}}) \\ \mathbf{C}_k &= \left[\mathbf{c}_k(\tau_1^{(k)}/N_s); \mathbf{c}_k(\tau_2^{(k)}/N_s); \cdots; \mathbf{c}_k(\tau_{M_k}^{(k)}/N_s)\right] \\ \overline{\mathbf{C}}_k &= \left[\overline{\mathbf{c}}_k(\tau_1^{(k)}/N_s); \overline{\mathbf{c}}_k(\tau_2^{(k)}/N_s); \cdots; \overline{\mathbf{c}}_k(\tau_{M_k}^{(k)}/N_s)\right] \\ \mathbf{N}(i) &= [\mathbf{n}(iN_s), \mathbf{n}(iN_s+1), \cdots, \mathbf{n}(iN_s+N_s-1)]\end{aligned}$$

where *diag* denotes a diagonal matrix having $\{\sqrt{P_i^{(k)}},\ i = 1, \cdots, M_k\}$ as its diagonal elements.

Use the **"fractional self-decorrelation" projector** for the kth user as

$$\mathbf{P}_k^{(p)} \stackrel{\text{def}}{=} \mathbf{I} - \mathbf{E}_k^{(p)}((\mathbf{E}_k^{(p)})^H \mathbf{E}_k^{(p)})^{-1}(\mathbf{E}_k^{(p)})^H \tag{4.5}$$

This $N_c M_c \times N_c M_c$ projector $\mathbf{P}^{(p)}$ projecting the time-sampled signal received at each antenna through this self-decorrelating projector $\mathbf{P}^{(p)}$,

$$\begin{aligned}\widetilde{\mathbf{X}}(i) &= \mathbf{X}(i)\mathbf{P}_k^{(p)} \\ &= \left\{\sum_{j \neq k}(\mathbf{A}_j \mathbf{\Gamma}_j \mathbf{C}_j b_i^{(j)} + \mathbf{A}_j \mathbf{\Gamma}_j \overline{\mathbf{C}}_j b_{i-1}^{(j)}) + \mathbf{N}(i)\right\} \mathbf{P}_k^{(p)}\end{aligned} \tag{4.6}$$

because $\mathbf{X}_k(i)\mathbf{P}_k^{(p)} = 0$. Note that this equation is true in a sense that the most dominant SOI (the kth user) energy is removed from $\mathbf{X}(i)$. $\widetilde{\mathbf{X}}(i)$, in

the proposed scheme, is to substitute $\{\mathbf{Y}_i^{(I+N)}\}$ to form the I+N correlation matrix $\widehat{\mathbf{K}}_i^{(I+N,ESO)}$. That is, signature sequence de-spreading process is no longer necessary to obtain $\widehat{\mathbf{K}}_i^{(I+N,ESO)}$. On the other hand, $\widehat{\mathbf{K}}_i^{(S+I+N,ESO)}$ is to remain as defined in the original algorithm Chen et.al. [1] , Wong et.al. [2] and Naguib et.al. [3].

That is, the $L \times N_s$ matrix $\widetilde{\mathbf{X}}_i^{(I+N)}$:

$$\widetilde{\mathbf{X}}_i^{(I+N)} \stackrel{\text{def}}{=} [\tilde{\mathbf{x}}(iT_b + T_s), \cdots, \tilde{\mathbf{x}}(iT_b + N_s T_s)]$$

Then form the two matrices,

$$\widehat{\mathbf{K}}_i^{(S+I+N,ESO)} \stackrel{\text{def}}{=} \mathbf{Y}_i^{(S+I+N)} (\mathbf{Y}_i^{(S+I+N)})^H \tag{4.7}$$

$$\widehat{\widetilde{\mathbf{K}}}_i^{(I+N,ESO)} \stackrel{\text{def}}{=} \widetilde{\mathbf{X}}_i^{(I+N)} (\widetilde{\mathbf{X}}_i^{(I+N)})^H, for 1 \leq i \leq I$$

The element-space-only beamforming weight vector $\mathbf{w}_i^{(ESO)}$ aims to maximize the SINR:

$$\begin{aligned} SINR &= \frac{\mathbf{w}^H \{\widehat{\mathbf{K}}_i^{(S+I+N,ESO)} - \widehat{\widetilde{\mathbf{K}}}_i^{(I+N,ESO)}\} \mathbf{w}}{\mathbf{w}^H \widehat{\widetilde{\mathbf{K}}}_i^{(I+N,ESO)} \mathbf{w}} \\ &= \frac{\mathbf{w}^H \widehat{\mathbf{K}}_i^{(S+I+N,ESO)} \mathbf{w}}{\mathbf{w}^H \widehat{\widetilde{\mathbf{K}}}_i^{(I+N,ESO)} \mathbf{w}} - 1 \end{aligned}$$

That is, the optimum weight vector is obtained as:

$$\mathbf{w}_i^{(ESO)} \stackrel{\text{def}}{=} \arg \max_{\mathbf{w}} \frac{\mathbf{w}^H \widehat{\mathbf{K}}_i^{(S+I+N,ESO)} \mathbf{w}}{\mathbf{w}^H \widehat{\widetilde{\mathbf{K}}}_i^{(I+N,ESO)} \mathbf{w}} \tag{4.8}$$

$\mathbf{w}_i^{(ESO)}$ is derived as the generalized eigenvector corresponding to the largest (in absolute value) generalized eigenvalue of the matrix pencil pair $\{\widehat{\mathbf{K}}_i^{(S+I+N,ESO)}, \widehat{\widetilde{\mathbf{K}}}_i^{(I+N,ESO)}\}$. This element-space-only (ESO) beamformer [1, 10, 11, 12, 23] implements a RAKE receiver with separable spatial processing and temporal processing.

From the use of fractional self-decorrelation pre-processing, $\widehat{K}_i^{(I+N,ESO)}$ is replaced by $\widehat{\widetilde{K}}_i^{(I+N,ESO)}$ which is a better estimation.

4.4 Physical Meaning of Fractional Self-Decorrelation Pre-processing

When the SOI and MAI's multipaths arriving at the base-station, the SOI's fingers occupy the whole symbol duration in the post-despreaded baseband data if the assumption made by Wong&Lok et.al.[2] is not applicable. The purpose of "fractional self-decorrelation" pre-processing is to remove the SOI's dominant-energy multipaths which spread the whole symbol duration from the received baseband data to give the approximated I+N components which are used to form the I+N spatial correlation matrix. In the linear filtering aspect, the fractional self-decorrelator rejects the SOI's multipaths with dominant energy, which means that it extracts the approximated SOI-free I+N components in raw baseband data. These I+N components are then used to form spatial correlation matrix for later on generalized eigen-decomposition. Like the case of self-decorrelator, the obtained I+N components are used to estimated the I+N components in raw baseband S+I+N data in terms of spatial correlation matrices, but not a direct estimation in time t or delay τ domains. This is because the multipaths of SOI are correlated with those of MAI in the real fading channel environment. Hence, only the approximated SOI's contribution and SOI-free I+N's contribution in the raw baseband data are obtained.

In the mathematical aspect, the fractional self-decorrelator is an eigen-subspace to reject the SOI's dominant-energy multipaths and ;hence, allow most of the I+N components and SOI's low-energy components to pass through. The fractional self-decorrelator $\mathbf{P}^{(p)}$ is not a complete null space; otherwise, it will reject everything including SOI, MAI and noise and there will be zero-energy output after the pre-processing of baseband data. In our scenario, the sum of the dimensions of SOI's eigen-subspace and I+N eigen-subspace is equal to the total dimensions of the space spanned by all discrete-time baseband data in a symbol duration. The eigen-subspace of SOI is orthogonal to that of I+N.

The reason why a certain number of largest eigenvectors is extracted from the column space of $\mathbf{S}$ in equation 4.3 to form the fractional self-decorrelator $\mathbf{P}^{(p)}$ is that the specified range of arrival time delays is not a priori known to the receiver. In the case of self-decorrelator , we know that the range of arrival time delays of SOI's multipaths is within a small fraction of the symbol duration. So, we could use all the possible time delayed versions of SOI's signature waveform up to the maximum possible delay spread. Therefore, we do not need to use the largest eigenvectors in the column space of $\mathbf{S}$ in equation 3.9 to form the self-decorrelator $\mathbf{P}^{\perp}$. Instead, the whole column space of matrix $\mathbf{S}$ in equation 3.9 is used to reject all possible SOI's multipaths. In the case of fractional self-decorrelator, the SOI's multipaths' arrival delays occupy the whole symbol duration. If all possible time-delayed signature waveforms are used to form the fractional self-decorrelator $\mathbf{P}^{(p)}$, $\mathbf{P}^{(p)}$ will become the null matrix which blocks everything including SOI, MAI and noise. Therefore, the best method is to use a certain number of largest eigenvectors in the column space of $\mathbf{S}$ to represent the SOI's eigen-subspace in which the SOI's dominant-energy multipaths lie in. The criteria for the selection of the value p in matrix $\mathbf{P}^{(p)}$ will be our further research interest.

4.5 Simulation Results

Monte Carlo simulations are used to verify the efficiency of the proposed fractional self-decorrelator technique, with the fading channel's delay spread equals a symbol period. Under such channel condition, the algorithms in [1, 10, 11, 12, 23] would be inapplicable. Therefore, the method used by Naguib et.al. [3]and the interference cancellation methods used by Liu & Geraniotis [5] and Luo & Blostein [6] are used to compare the performance of the proposed method, which verify that the fractional decorrelation technique gives a notable improvement in the case of the multiple delay spread approaching the

symbol period and without "doubling" the channel capacity mentioned earlier in section 2.2.

The simulation below demonstrates the significant improvements effected for the blind ESO version of the original methods in [10, 11, 12]. The "fractional self-decorrelator" is implemented with $p = 60$.

All simulations below involves a uniform half-wavelength-spaced linear array of 6 identical omni-directional antennas with no mutual coupling. 127-chip Gold codes are used as spreading sequences (with cross-correlation $r^{(j,k)} = r$ among sequences at 0.4, unless otherwise stated) for the BPSK data symbol sequences, which are independent over time and among the sources. $L = 2$. The multipath carrier phase shift, $\gamma_{m_k}^{(k)}$ is uniformly distributed in $(0, \pi]$ and independent across all multipaths and from trial to trial. The SOI has a direct path arrives from 0° from the broadside and a delayed path arriving from 15° from the broadside with an arrival delay that varies randomly from run to run with uniform distribution from 0 to $127 * L - 1$ (within one symbol duration)integral number of time samples. There exist 3 interfering sources, each with direct and delayed paths respectively from $-25°$ and 25°, $-57°$ and 82°, 57° and 17°. Each of these 6 interfering multipaths has an arrival delay that is randomized from run to run between 0 and $127 * L - 1$(within a symbol period) integral number of time samples. A synchronous model with perfect chip synchronization is assumed for the direct path. All SNR figures in all figures are computed with respect to the SOI's direct path. The delayed path is always $-6dB$ weaker in power than the direct path from the same source, whether the source is the SOI or an interference. All SIR figures in all figures are computed for the direct path of an individual interfering source with respect to the SOI's direct path; and each interfering source has SIR equal $-5dB$. Also plotted in each figure is the hypothetical (and optimum, with respect to beamforming) case where no SOI energy exists in the I+N segment. Other details are listed in each figure's caption. Unless stated otherwise, each data point represents

the mean of 300 independent Monte Carlo experiments.

Fig.4.1 plots the magnitude distribution of the singular values of **S**. It shows there exists a natural cut-off points in the selection of p. This means that there exists a certain number of eigenvectors dominant to the rest in the column space of matrix **S**. Fig.4.2 plots the spatial beam pattern for one particular Monte Carlo experiment comparing the proposed "blind" space-time processing method with that in [3, 21]. Fig.4.3 plots the spatial beam pattern comparing the proposed "blind" space-time processing method with that in [5, 6]. The proposed method places a higher beamformer peak over the arrival angles of *both* paths of the SOI but deeper nulls against the interference. Relative to the ideal but hypothetical case where no SOI energy exists in the I+N data group, the proposed method produces the best possible SOI constructive summation band interference rejection for the given antenna array.

The beamformer output SINR's for the proposed method and the method in (Naguib et.al. & Suard et.al.) [3, 21] are respectively 83% and 53% of the ideal case where there is no SOI energy existing in the I+N data group, for 300 independent Monte Carlos runs. For the interference cancellation methods used by Liu & Geraniotis [5] and Luo & Blostein [6], the simulation result shows that their output SINR are 41% and 37% of the ideal case respectively. This shows that the proposed fractional self-decorrelation pre-processing not only has a substantial improvement compared with Naguib et.al. [3]'s method, but also it has a comparable performance with Liu & Geraniotis [5] and Luo & Blostein [6].

Fig.4.4, plotting the beamformer's SINR versus the input SIR (defined above), shows the proposed " fractional self-decorrelator" pre-processing technique consistently improves the method in (Naguib et.al. & Suard et.al.) [3, 21] by 2 to 4 dB. Compared with the proposed algorithm, the interference cancellation methods developed by Liu & Geraniotis [5] and Luo & Blostein [6] are consistently worse by about 3 to 6 dB.

Fig.4.5, plotting the beamformer's SINR versus the input SNR (defined above), shows the proposed technique consistently improves the method in (Naguib et.al. & Suard et.al.) [3, 21] by 2 to 6 dB. The methods developed by Liu & Geraniotis [5] and Luo & Blostein [6] are consistently worse than the proposed method by about 1 to 6 dB.

Fig.4.6, plotting the beamformer's output SINR versus the spreading sequences' cross-correlation coefficients, shows the proposed technique's improved robustness against the near-far problem from another perspective. This figure shows clearly that the drop off point of the curves in other methods mentioned above are lower than the proposed method when the cross-correlation r approaches to 1. There is a 3 dB lower in Suard et.al.[21] and Naguib et.al. [3] cases while there is a 4 dB lower in Liu & Geraniotis [5] and Luo & Blostein [6] methods. Also, the proposed method's performance is consistently better than the method by Naguib et.al. [3] from 3 to 12 dB while there is a comparable performance of the proposed method compared with Liu & Geraniotis [5] and Luo & Blostein [6] cases.

Fig.4.7 plots the beamformer's output SINR versus the number of p of eigenvectors used in defining the self-decorrelating projection matrix $\mathbf{P}^{(p)}$. As p increases, the MAI and noise in the I+N data group becomes a poorer estimate for the MAI and noise in the S+I+N data group. Therefore, this lowers the beamforming performance.

Below are the eight graphs showing the above details.

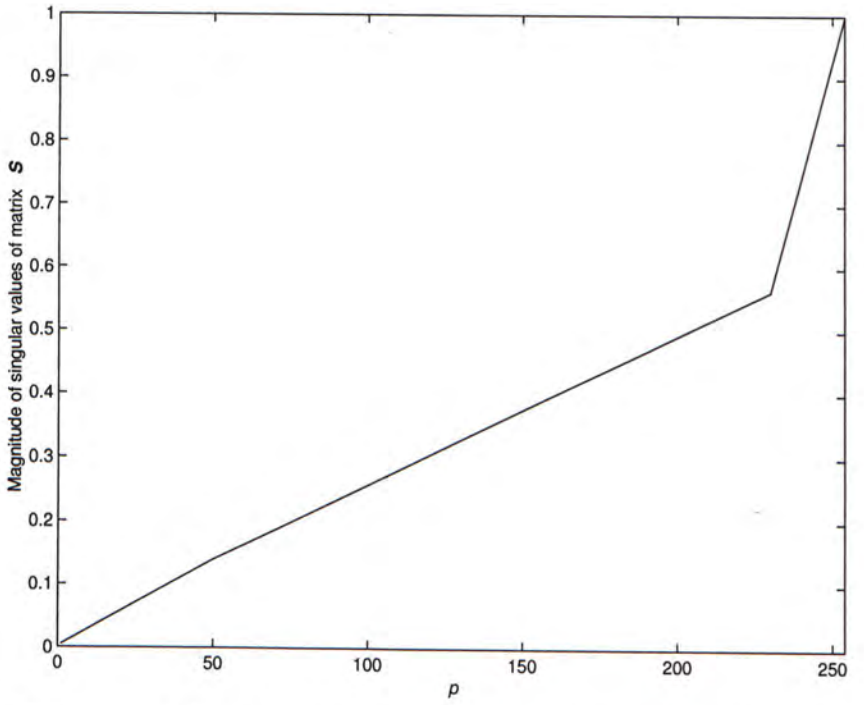

Figure 4.1: Magnitude distribution of the singular value of **S**

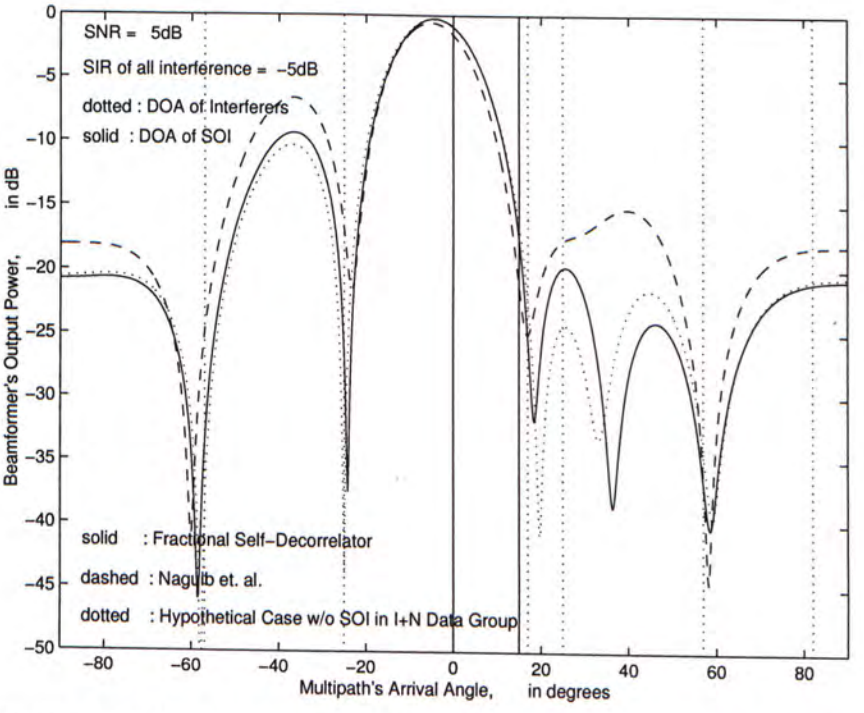

Figure 4.2: Beam patterns for various methods — SNR = 5dB.

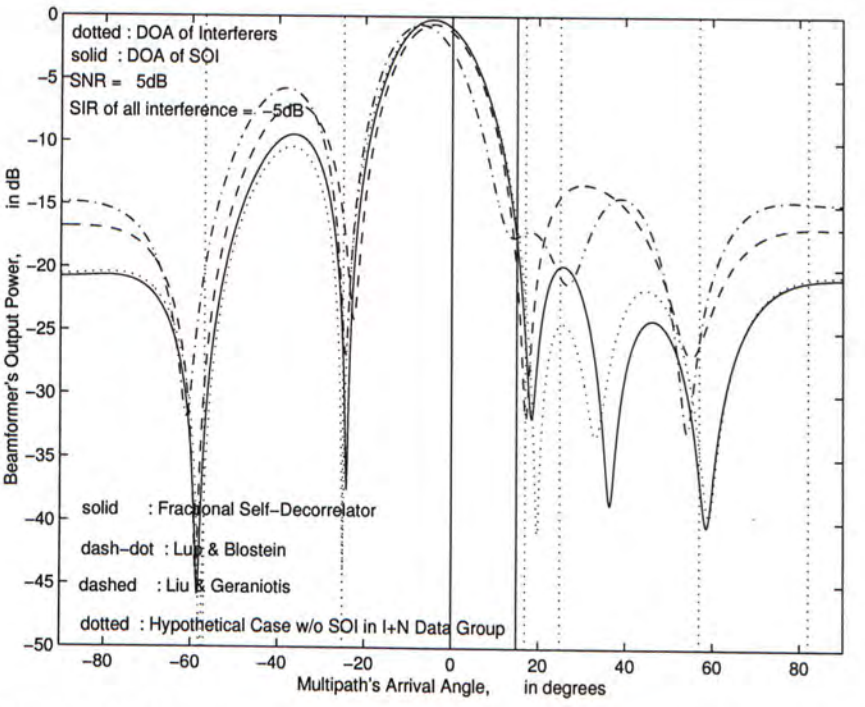

Figure 4.3: Beam patterns for various methods — SNR = 5dB.

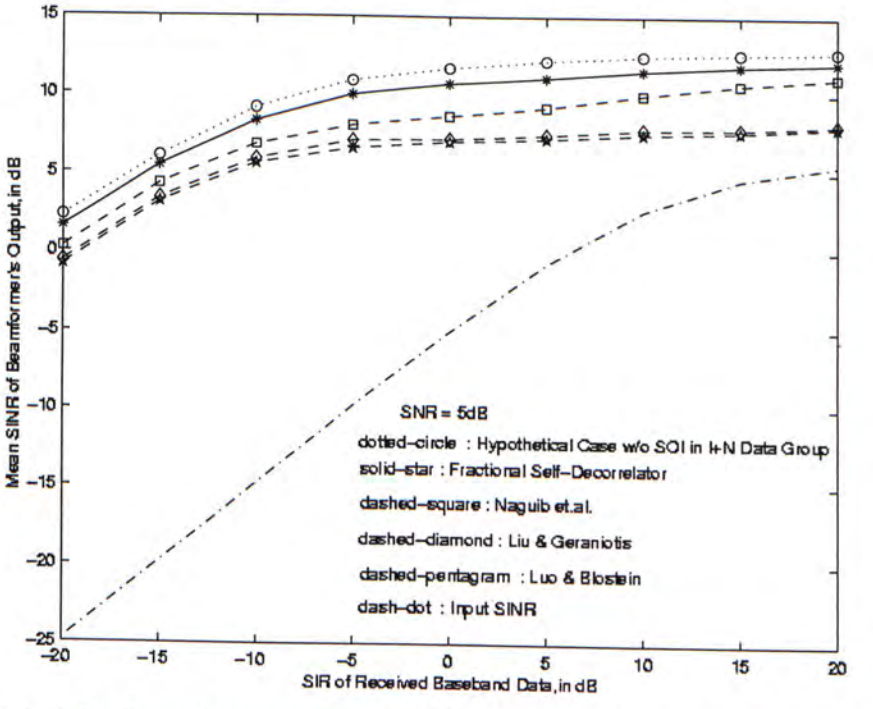

Figure 4.4: The beamformer output's SINR versus the de-spreading filter input's SIR, for various methods — same scenario as in Fig.4.2.

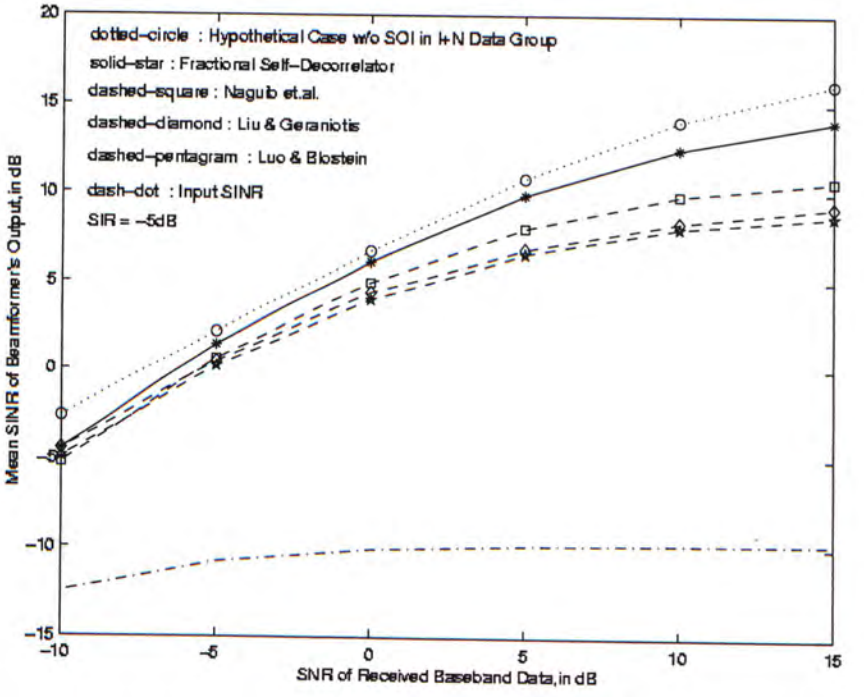

Figure 4.5: The beamformer output's SINR versus the de-spreading filter input's SNR, for various methods — SIR = −5dB but otherwise same scenario s in Fig.4.2.

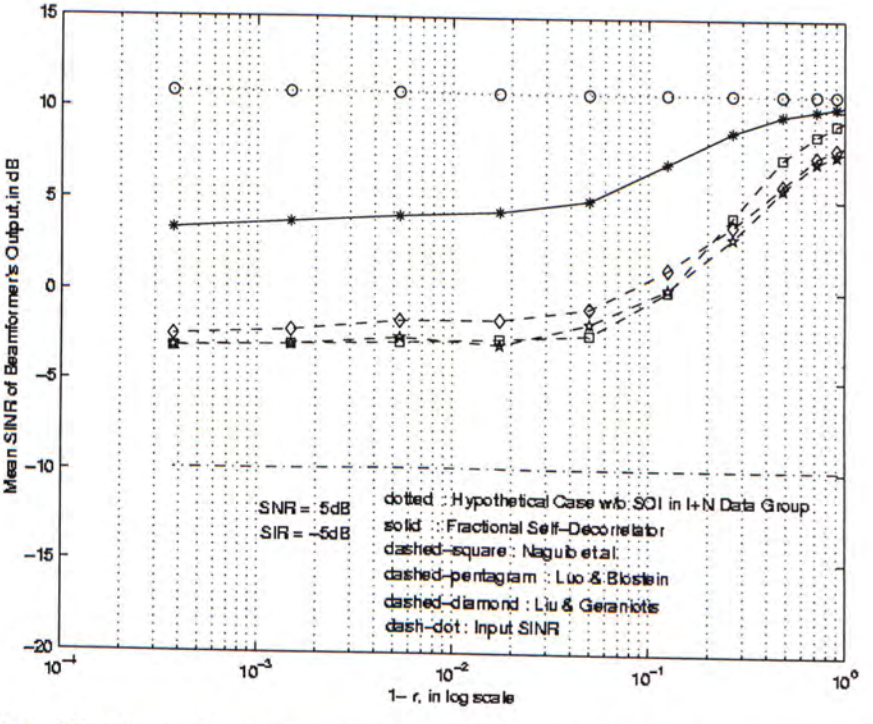

Figure 4.6: The beamformer output's SINR versus the cross-correlation coefficient among spreading sequences, for various methods — same scenario as in Fig.4.2.

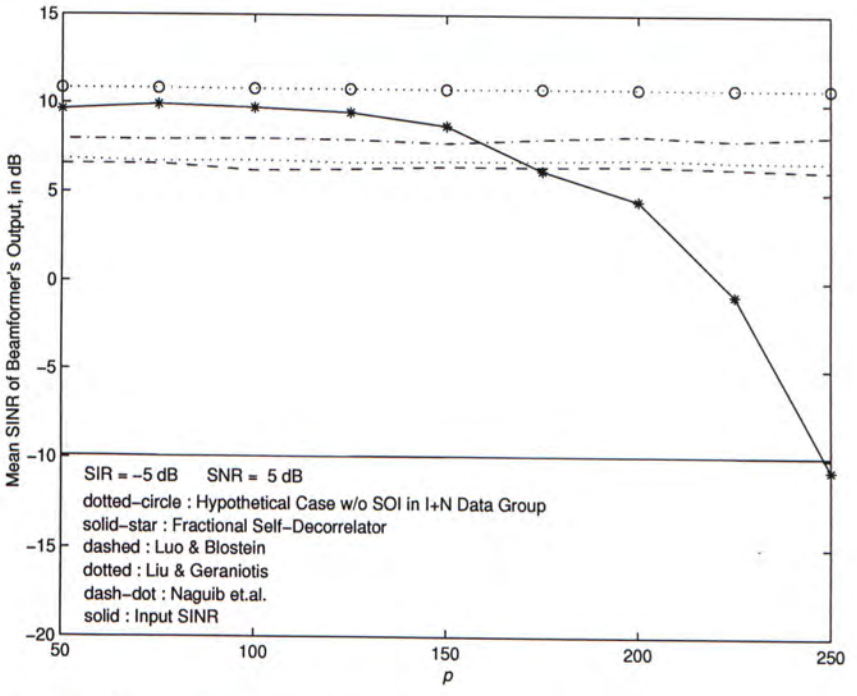

Figure 4.7: The beamformer output's SINR versus the number of eigenvectors used in the self-decorrelating projection matrix $\mathbf{P}^{(p)}$ — same scenario as in Fig.4.2.

	1^{st} path	2^{nd}path
Arrival angles of SOI's multipaths	$0°$	$15°$
Arrival angles of 3 MAI's multipaths	$-25°$	$25°$
	$-57°$	$82°$
	$57°$	$17°$
Arrival time delays of SOI's multipaths	0 chips	randomized within the whole symbol interval
Arrival time delays of 3 MAI's multipaths	randomized within the whole symbol interval	randomized within the whole symbol interval
SIR	$-5dB$	$6dB$ weaker than 1^{st} path
SNR	$5dB$	$6dB$ weaker than 1^{st} path
cross-correlation among all users' signature sequences r	0.4	
number of time samples per chip M_c	2	
number of largest eigenvectors chosen p	60	
A half-wavelength-spaced uniform linear array with 6 antenna elements with no mutual coupling		

Table 4.1: Summary list of parameter values from figures 4.2 to 4.7

Chapter 5

Complexity Analysis and Schematics of Proposed Techniques

5.1 Computational Complexity

5.1.1 Self-Decorrelation Applied in Element-Space-Only (ESO) RAKE Receiver

Assume the $L \times 1$ baseband measurement at time t equals:

$$\begin{aligned}\mathbf{x}(t) = \; & \sum_{k=1}^{K} \sum_{m_k=1}^{M_k} \sqrt{P_{m_k}^{(k)}} \mathbf{a}(\theta_{m_k}^{(k)}) \sum_{i=0}^{I} \{ b_i^{(k)} u(t - iT_b - \tau_{m_k}^{(k)}) \\ & c_k(t - iT_b - \tau_{m_k}^{(k)}) e^{j\gamma_{m_k}^{(k)}} \} + \mathbf{n}(t) \end{aligned} \tag{5.1}$$

which is the same as Eq.(3.1). In the computational analysis, we assume the number of chips of each multiple access user's spreading sequence is N_c and M_c samples are taken per chip period. Therefore, we denote $N_s = N_c * M_c$ which stands for the total number of time samples within a symbol period.

After the baseband signal is received, it is passed through the matched filter of the (kth) desired user, $h_k[n] = h_k(nT_c/M_c)$.

A) Computational requirement by the original algorithm [1]

The computational requirement of the matched filtering process is $4N_bN_s(N_s-1)$ real addition and $2N_bN_sN_s$ real multiplication by assuming that the received baseband signal has I & Q components represented by complex numbers. We assume that N_b symbol intervals are considered.

After the received baseband signal is passed through the matched filter of the desired user, each symbol interval can be divided into two segments.They are the S+I+N segment containing much of the SOI energy and the I+N segment which is away from the "fingers" duration.Hence, the two spatial correlation matrix $\widehat{\mathbf{K}}_i^{(S+I+N)}$ and $\widehat{\mathbf{K}}_i^{(I+N)}$ are formed by the two segments in the delay τ domain respectively.

When forming spatial correlation matrix $\widehat{\mathbf{K}}_i^{(S+I+N)}$, we assume the multipath delay spread is D chips and we have DM_c samples in the duration of "fingers" in each symbol interval. Therefore , we need $4(DM_cN_b-1)LL$ real addition and $(DM_cN_b)LL$ real multiplication. Since the matrix $\widehat{\mathbf{K}}_i^{(S+I+N)}$ is Hermitian, there are $4(DM_cN_b-1)L!$ real addition and $4(DM_cN_b)L!$ real multiplication needed to form the matrix.

Similarly, for the spatial correlation matrix $\widehat{\mathbf{K}}_i^{(I+N)}$, we need $4(N_b(N_s-DM_c)-1)L!$ real addition and $(4N_b(N_s-DM_c))L!$ real multiplication when using the delay segment away from the "fingers" segment.

B) Computational requirement by using the self-decorrelation pre-processing

We need $4N_bDM_c(N_s-1)$ real addition and $2N_bDM_cN_s$ real multiplication in the matched filtering process since it is assumed that the multipath delay spread is D chips. This is the same as the original algorithm mentioned above.

For each symbol interval, the total number of time samples is $N_s = N_c * M_c$. Therefore, the size of the self-decorrelation projector is $N_s \times N_s$.

When the raw received baseband signal is passed through the self-decorrelation pre-processing, we need $4N_s(N_s-1)$ real addition and $4N_sN_s$ real multiplication *per symbol interval.*

After the matched filtering process, the received baseband signal forms S+I+N data group in the "fingers" segment in each symbol interval. The spatial correlation matrix $\widehat{\mathbf{K}}_i^{(S+I+N)}$ is formed. After the self-decorrelation pre-processing to the received baseband signal, the spatial correlation matrix $\widehat{\mathbf{K}}_i^{(I+N)}$ is formed by using the I+N data group within the whole symbol interval in the time t domain.

The two spatial correlation matrix block size is $L \times L$, where L is the number of elements in the antenna array.

Also, we assume N_b symbol intervals are considered when forming the two spatial correlation matrix.

Therefore, when forming the spatial correlation matrix $\widehat{\mathbf{K}}_i^{(S+I+N)}$, the computational steps are the same as the original algorithm.That is , there are $4(DM_cN_b-1)L!$ real addition and $4(DM_cN_b)L!$ real multiplication.

For the spatial correlation matrix, $\widehat{\mathbf{K}}_i^{(I+N)}$, we need $(4(N_sN_b-1))L!$ real addition and $(4N_sN_b)L!$ real multiplication.

C) Extra steps needed

When we consider the Element-Space-Only(ESO) RAKE receiver, the use of self-decorrelation pre-processing algorithm leads to the additional computation steps which include $2N_b(DM_c+N_s)N_s+4N_bDM_cL!$ real multiplication and $4N_bDM_c(N_s-1)+4(N_bDM_c)L!$ real addition compared with the original algorithm by Chen et.al. [1]. So, there are extra $2(DM_c+N_s)N_s+4DM_cL!$ real multiplication and $4DM_c(N_s-1)+4(DM_c)L!$ real addition operations per symbol period.

5.1.2 Fractional Self-Decorrelation Applied in Element-Space-Only (ESO) RAKE Receiver

A) Method proposed by Naguib et.al. [3] and Suard et.al. [21]

When the received baseband signal is passed through the matched filter, the S+I+N data group is formed and it needs $4(N_s - 1)N_sN_b$ real addition and $2N_sN_sN_b$ real multiplication during the process. The duration of both S+I+N and I+N data groups are the whole symbol interval which includes $N_s = N_c * M_c$ data samples, unlike the proposed algorithm by Chen et.al. [1], which the symbol interval can be divided into two segments representing the S+I+N and I+N data group respectively.

In the algorithm of Naguib et.al. [3], I+N data group is the received baseband signal itself.

Therefore, for the formation of spatial correlation matrix $\widehat{\mathbf{K}}_i^{(I+N)}$, it requires $4(N_sN_b - 1)L!$ real addition and $4N_sN_bL!$ real multiplication.

Similarly, for the formation of $\widehat{\mathbf{K}}_i^{(S+I+N)}$ spatial correlation matrix, it also needs $4(N_sN_b - 1)L!$ real addition and $4N_sN_bL!$ real multiplication.

B) Interference Cancellation Method proposed by Luo & Blostein [6]

Since the received baseband signal needs to be despreaded, it needs $4(N_s - 1)N_sN_b$ real addition and $2N_sN_sN_b$ real multiplication during the process to form S+I+N data group.

The received baseband signal also needs to be despreaded by the orthogonal matched filter for the interference cancellation purpose.So, it also needs $4(N_s - 1)N_sN_b$ real addition and $2N_sN_sN_b$ real multiplication.

If we consider N_b symbol intervals , it needs $4(N_sN_b - 1)L!$ real addition and $4N_sN_bL!$ real multiplication to form the spatial correlation matrix $\widehat{\mathbf{K}}_i^{(S+I+N)}$.

Similarly, it requires $4(N_sN_b - 1)L!$ real addition and $4N_sN_bL!$ real multiplication to form the spatial correlation matrix $\widehat{\mathbf{K}}_i^{(I+N)}$.

C) Interference Cancellation Method proposed by Liu & Geraniotis [5]

In the algorithm proposed by Liu & Geraniotis [5], the S+I+N data group is also formed by passing the received baseband signal through the matched filter of the desired user. It requires $4(N_s-1)N_sN_b$ real addition and $2N_sN_sN_b$ real multiplication.

Also, the received baseband signal is needed to pass through the orthogonal matched filter for interference cancellation purpose.It needs $4(N_s-1)N_sN_b$ real addition and $2N_sN_sN_b$ real multiplication.

Assumed that N_b symbol intervals are considered, it requires $4(N_sN_b-1)L!$ real addition and $4N_sN_bL!$ real multiplication to form the spatial correlation matrix $\widehat{\mathbf{K}}_i^{(S+I+N)}$.

Similarly, it requires $4(N_sN_b - 1)L!$ real addition and $4N_sN_bL!$ real multiplication to form the spatial correlation matrix $\widehat{\mathbf{K}}_i^{(I+N)}$. The computational operations needed are the same as Luo & Blostein [6].

D) The proposed Fractional Self-Decorrelation Pre-processing

For the proposed fractional self-decorrelation pre-processing method, the received baseband signal is first passed through the matched filters in each antenna elements to form S+I+N data group so it requires $4(N_s-1)N_sN_b$ real addition and $2N_sN_sN_b$ real multiplication, which is the same as the methods mentioned above.

The fractional self-decorrelation pre-processing is like an orthogonal eigen-subspace projector with size $N_s \times N_s$. When the received baseband data is passed through it, $4N_s(N_s-1)$real addition and $4N_sN_s$ real multiplication are needed per symbol period.

After the received baseband signal is passed through the proposed subspace projector, the most significant SOI energy is removed and hence I+N data group is formed.

The spatial correlation matrix $\widehat{\mathbf{K}}_i^{(S+I+N)}$ is formed by requiring $4(N_s N_b - 1)L!$ real addition and $4N_s N_b L!$ real multiplication if N_b symbol periods are considered.

For the spatial correlation matrix $\widehat{\mathbf{K}}_i^{(I+N)}$, it needs $4(N_s N_b - 1)L!$ real addition and $4N_s N_b L!$ real multiplication.

E) Comparison among all the methods

Compared with the method suggested by Naguib et.al. [3], the proposed algorithm needs extra $4N_s(N_s - 1)N_b$ real addition and $4N_s N_s N_b$ real multiplication operations if N_b symbol periods are considered.

If the proposed fractional self-decorrelation pre-processing is compared with Luo & Blostein [6] and Liu & Geraniotis [5], there are extra $2N_s N_s N_b$ real multiplication operations needed.

Therefore, the extra computational steps when the proposed method is used are $4N_s(N_s - 1)$ real addition and $4N_s N_s$ real multiplication per symbol interval, compared with Naguib et.al. [3]. There are additional $2N_s N_s$ real multiplication operations per symbol period if we compare the proposed method with Luo & Blostein [6] and Liu & Geraniotis [5].

5.2 Schematics of the Two Proposed Techniques

Figure 5.1: Detailed schematics of Self-Decorrelation technique

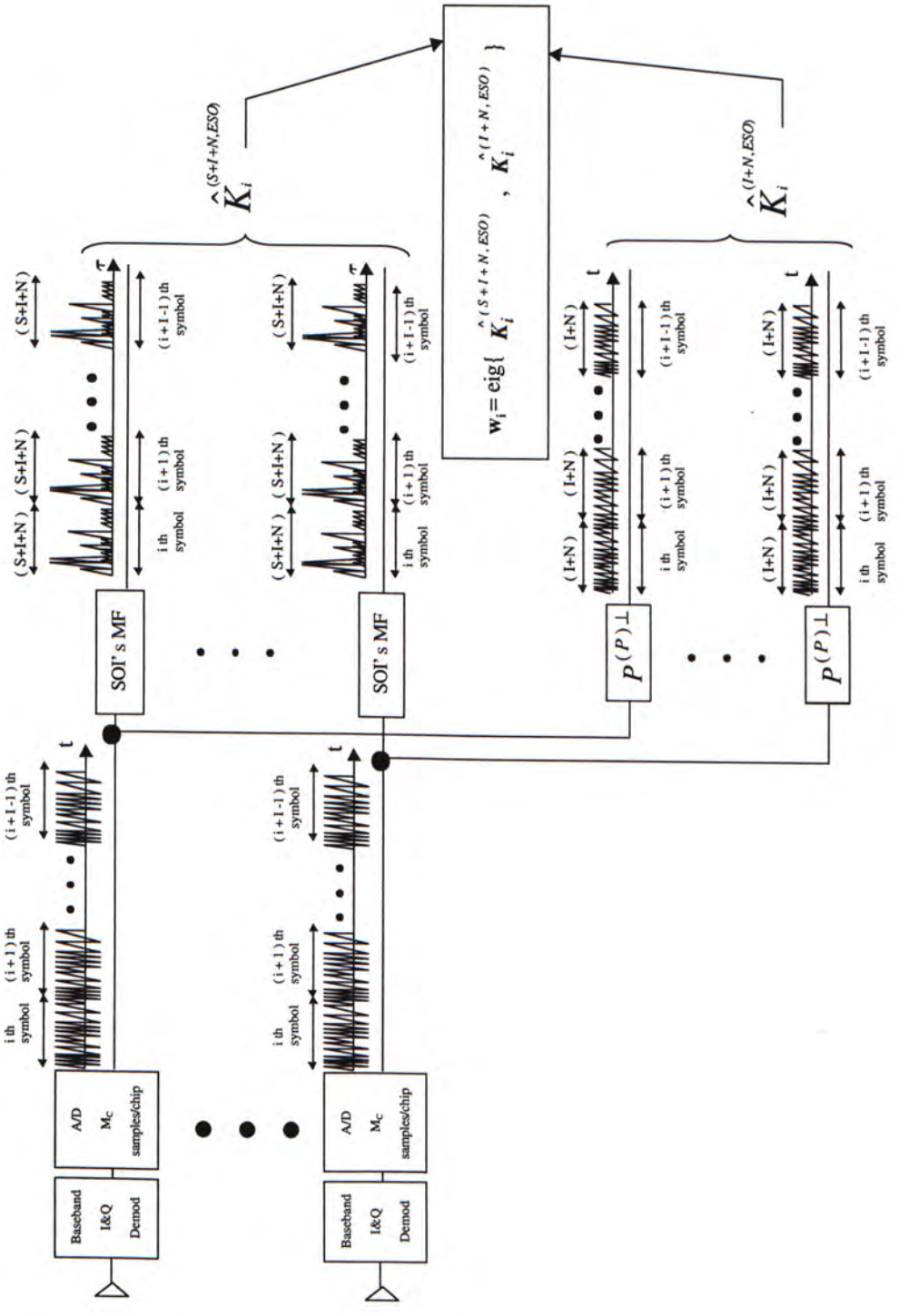

Figure 5.2: Detailed schematics of Fractional Self-Decorrelation technique

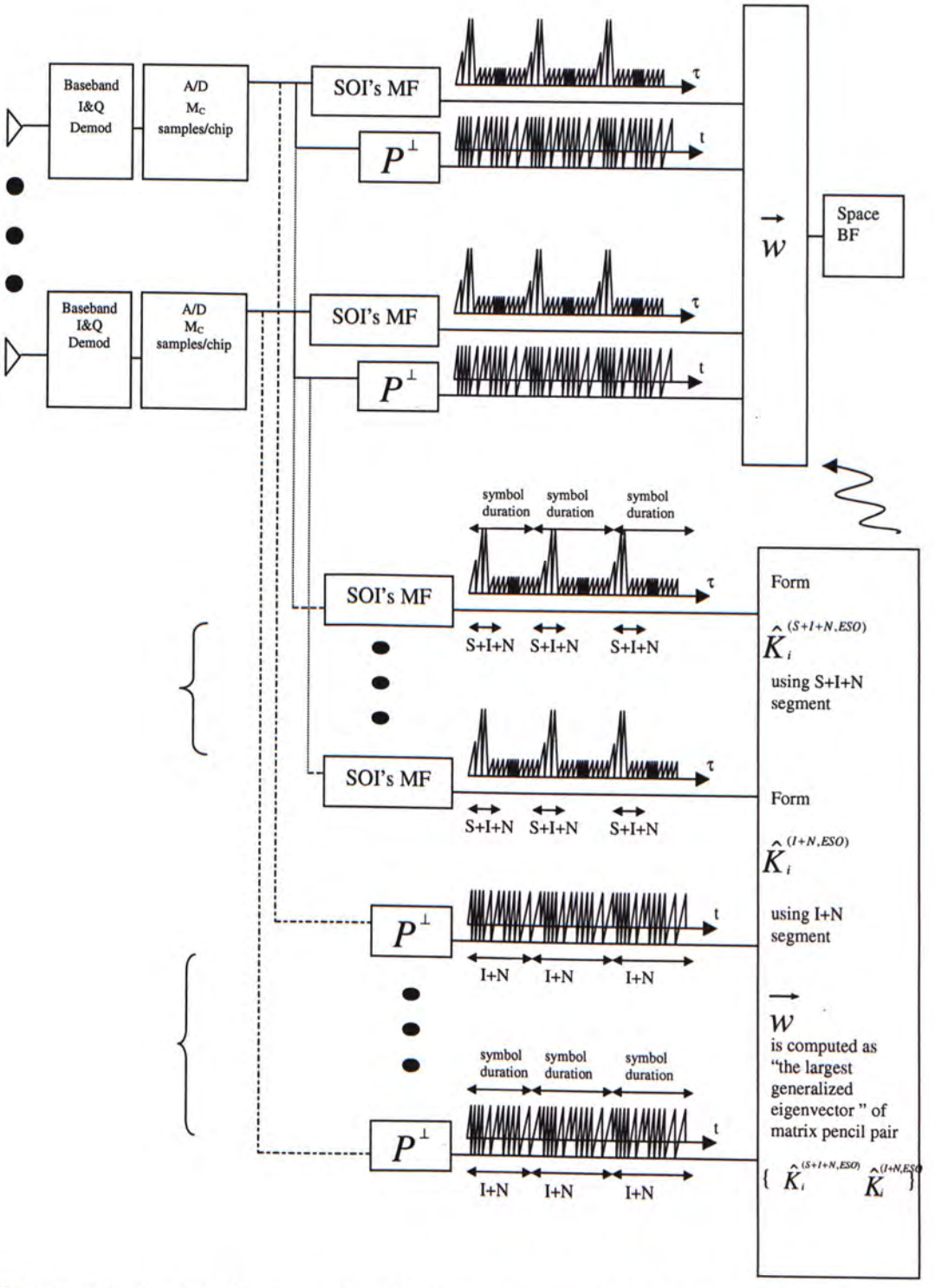

Figure 5.3: Detailed schematics of Element-Space-Only(ESO) RAKE receiver with Self-Decorrelation technique

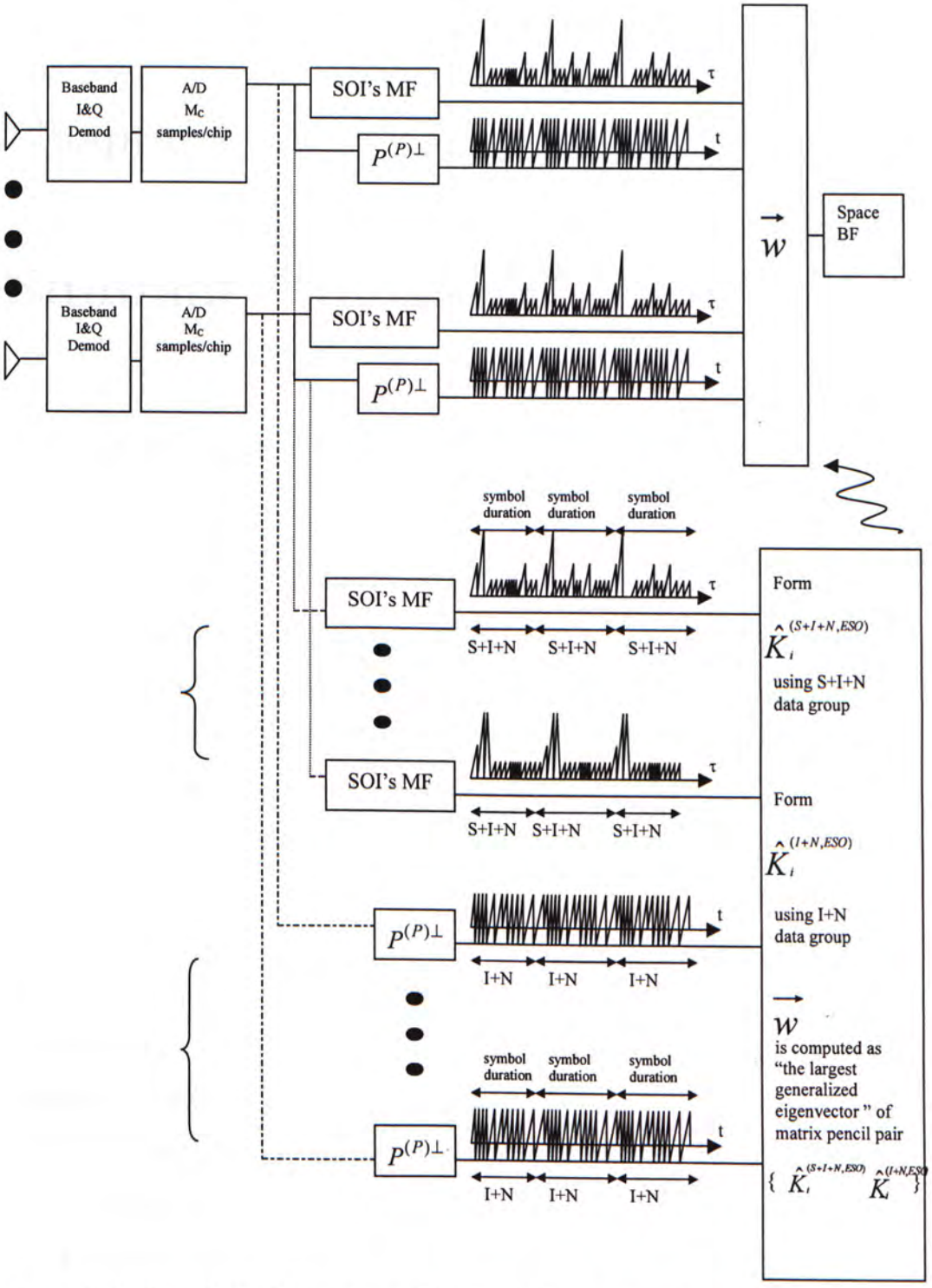

Figure 5.4: Detailed schematics of Element-Space-Only(ESO) RAKE receiver with Fractional Self-Decorrelation Pre-processing

Chapter 6

Summary and Conclusion

6.1 Summary of the Thesis

In the thesis, a class of signal processing schemes developed in Naguib et.al. [3] & Suard et.al. [21], Liu & Zoltowski [4], Wong et.al. [2], Chen et.al. [1], Liu & Geraniotis [5] and Luo & Blostein [6] have been reviewed.

These schemes are applied to the family of maximum-SINR blind space-time RAKE receiver for DS-CDMA where the single-user-type detectors are used. These types of receivers are used to tackle the "near-far" problem existing in the single-user-type detectors.

The significance of this family of blind space-time receivers is that (1) the channel's multipath arrival angle or arrival delay or power profile are not necessarily estimated [1] , (2) knowledge of the receiver's nominal or actual antenna array manifold is not needed and (3) only the desired user's signature sequence is required.This is an advantage for downlink because the mobile handset would only need its own signature sequence but not the other users' signature sequence.

[1]No non-information symbol sequence for training is needed.

6.1.1 The Self-Decorrelation Pre-processing Technique

In Naguib et.al.[3] and Suard et.al.[21], the raw received baseband signal is passed through the desired user's matched filters. The output of the matched filters is the S+I+N data group which is then used to form the S+I+N *spatial* correlation matrix. For the formation of I+N *spatial* correlation matrix, the un-despreaded received data, I+N data group ,is used. This scheme separates the spatial and temporal processing, which is thus incapable to make good use of the fading channel's two-dimensional space-time structure.

In Liu & Zoltowski [4], an extended scheme which uses both spatial and temporal information is proposed. The S+I+N *space-time* correlation matrix is formed by using the despreaded output, S+I+N data group while I+N *space-time* correlation matrix is formed by using the un-despread recevied data, I+N data group. Since there is a multipaths' arrival delay temporal structure change when the received baseband data is passed through the temporal despreading filter, this means that the I+N data group is a poor estimation for the interference and noise corrupting the S+I+N data group. Hence, the resulted beamformer's weight vector is not well-estimated.

In Wong et.al. [2] and Chen et.al. [1], the problem that there is a change in temporal structure in the above scheme is alleivated. There is an assumption that the multipath arrival delay spread is within a small fraction of a symbol duration, such as IS-95 standard. The S+I+N data group is formed from the despreading filter's output during the delay segment in each symbol's period containing the cluster of "fingers" while the remaining delay segment is used to form the I+N data group. So, both S+I+N and I+N data groups are in the delay τ domain.

However, there is a common problem in the three schemes that a significant or even a trace of SOI's energy exists in the I+N data group. This means that the estimated beamformer will reject a significant portion of the desired

signal and receive the multiple access interference. In the thesis, a novel self-decorrelation technique is proposed to perform the pre-processing before the despreading filter so that there is no SOI's energy left in the I+N data group. The self-decorrelator is the orthogonal space with reference to the vector space spanned by the desired signature sequence and its time-delayed versions up to the duration of the cluster of "fingers" within a symbol interval. Therefore, the trace of SOI energy due to the non-zero lag autocorrelation in delay domain would be removed. The more accurate I+N data group is estimated.

In the simulation, the self-decorrelation technique is applied at the simplest beamforming version, the element-space-only version of this family of receivers developed in Wong et.al. [2] and Chen et.al. [1].

From the simulation, the self-decorrelation technique shows a significant improvement over the scheme proposed by Chen et.al. [1], which means that there is a need to remove all SOI energy in I+N delay segment(I+N data group) in order to give good estimation to the interference and noise corrupting the S+I+N data group.

6.1.2 The Fractional Self-Decorrelation Pre-processing Technique

In Chen et.al. [1] and Wong et.al. [2], it is necessary to have the assumption that the multipath delay spread in the fading channel is within a small fraction of a symbol duration. However, there is a substantial demand in the speed of data rate for the next generation wireless communication which makes this assumption inappliciable. Therefore, in the thesis, a novel fractional self-decorrelation pre-processing which extends the idea of self-decorrelation is proposed under the assumption that the multipath delay spread approaches the *whole symbol duration.*

The proposed fractional self-decorrlation pre-processing is the orthogonal

eigen-subspace which is orthogonal to the eigen-subspace spanned by selecting a certain number of largest singular-value column vectors in the matrix S_k in equation 4.3 which stores all possible time-delayed signature waveforms occupying the whole symbol duration. This self-decorrelator is with arbitary dimension but not equal to the full dimension spanned by using all the time samples in a symbol interval. After the received baseband data is passed through the orthogonal eigen-subspace, a significant portion of SOI's dominant energy is removed. The output of the fractional self-decorrelator is the approximated SOI-free I+N data group.

This pre-processing scheme has significant advantage over the schemes proposed by Liu & Geraniotis [5] and Luo & Blostein [6]. In their work, it is necessary to have an orthogonal signature sequence corresponding to each of the desired user's spreading sequence for interference cancellation, which means *doubling* the channel capacity occupied by each multiple access user. Also, the schemes proposed by Chen et.al. [1] and Wong et.al. [2] could not be applied since the multipath delay spread occupies the whole symbol duration.

Since the schemes developed in Chen et.al. [1] and Wong et.al. [2] are inappliciable, the simulation results will compare the various performance of the proposed fractional self-decorrelation pre-processing , Naguib et.al.[3]'s scheme , Liu & Geraniotis [5]'s scheme and Luo & Blostein [6]'s scheme.

The proposed technique is applied in the Element-Space-Only (ESO) beamforming version of the family of maximum-SINR blind space-time RAKE receivers in Chen et.al. [1] and Wong et.al. [2] in the simulation experiments.

From the simulation results, the fractional self-decorrelation pre-processing shows a comparable performance with Liu et.al. [5] and Luo et.al. [6]. Also, there is a significant improvement, about 30 % better than Naguib et.al. [3] scheme which there is a significant SOI energy in the I+N data group.

6.2 Conclusion

Two novel self-decorrelation pre-processings are proposed. They are fundamentally different to the well-known decorrelating detector which requires all multiple access users' spreading sequences and the estimated cross-correlation coefficients among the users. For the two proposed self-decorrelation pre-processings, only the desired user's signature sequence is a priori known. The self-decorrelator is a projection matrix corresponding to the orthogonal subspace which is orthogonal to the SOI's subspace spanned by all possible time-delayed versions of the desired user's signature sequences up to the duration of "fingers" in the post-despread baseband data. The fractional self-decorrelation pre-processing is the projection matrix which is the orthogonal eigen-subspace orthogonal to the SOI's eigen-subspace spanned by selecting a certain number of the largest singular-value column vectors in the column space of S_k in equation 4.3. They aim to remove the irreducible error floor existing in the single-user-type detector in DS-CDMA at high SNR as shown in the simulation results.

6.3 Future Work

The theoretical performance analysis of these two pre-processing techniques is being conducted. The journal version of the work will involve both the statistical analysis of the two proposed techniques and how these two proposed techniques are used in the family of receiver architectures proposed by Chen et.al. [1], which includes the Blind Element-Space-Only, Blind Element-Space/Delay,Blind Element-Space/Delay-DFT and Blind Beamspace/Delay-DFT RAKE receivers.

The criteria for selecting the value of p in fractional self-decorrelator $\mathbf{P}^{(p)}$ will be investigated. It is predicted that it will depend on the number of

interfering sources and the value of cross-correlation between SOI's multipaths and MAI's mulitpaths, which means that how severe the near-far problem is. This is because the value of p classifies the whole vector space spanned by all the time-samples in a symbol duration into SOI's eigen-subspace, MAI's eigen-subspace and noise's subspace. The derived SOI's eigen-subspace, MAI's eigen-subspace and noise's eigen-subspace are orthogonal to each other. This classification depends on the value of p which might be changed due to the cross-correlation among the SOI and MAI's multipaths in real fading channel environment.

In the two proposed pre-processing techniques, a priori known of the SOI's multipath delay spread is needed. We will find out this priori knowledge from the output of the pre-processing so that this priori knowledge could be known at the receiver side in advance. Hence, an appropriate self-decorrelator is adopted with different assumptions to maintain good BER performance.

Bibliography

[1] Y. F. Chen, M. D. Zoltowski, J. Ramos, C. Chatterjee, and V. Roychowdhury, " Reduced-Dimension Blind Space-Time 2-D RAKE Receivers for DS-CDMA Communication Systems," *IEEE Trans. Signal Processing*, vol. 48, pp. 1521–1536, June 2000.

[2] T. F. Wong, T. M. Lok, J. S. Lehnert, and M. D. Zoltowski, " A Unified Linear Receiver for Direct-Sequence Spread-Spectrum Multiple Access Systems with Antenna Arrays and Blind Separation," *IEEE Trans. Information Theory*, vol. 44, pp. 659–676, Mar. 1998.

[3] A. Naguib, A. Paulraj, and T. Kailath, " Capacity Improvements with Basestation Antenna Arrays in Cellular CDMA," *IEEE Trans. Vehicular Technology*, vol. 43, pp. 691–698, Aug. 1994.

[4] H. Liu and M. D. Zoltowski, " Blind Equalization in Antenna Array CDMA Systems," *IEEE Trans. Signal Processing*, vol. 42, pp. 161–172, Jan. 1997.

[5] S. C. Liu and E. Geraniotis, " Low-Complexity Fast-Convergence Blindly Adaptive Array Processing Techniques for Wideband CDMA Networks," *IEEE Global Telecommunications Conference*, pp. 3308–3313, 1998.

[6] T. Luo and S. D. Blostein, " Using Signal Cancelation for Optimum Beamforming in a Cellular CDMA System," *IEEE Intl. Conf. Acoustics,Speech & Signal Processing*, pp. 2493–2496, 1998.

[7] K. T. Wong, G. Liao, S. K. Cheung, M. D. Zoltowski, J. Ramos, and P. C. Ching, " A "Self-Decorrelating" Technique to Enhance Blind Space-Time RAKE Receivers with Single-User-Type DS-CDMA Detectors," *IEEE Intl. Conf. Communications*, vol. 5, pp. 1491–1495, 2001.

[8] K. T. Wong and S. K. Cheung, " "Fractional Self-Decorrelation" Preprocessing to Enhance the Output SINR of Single-User-Type DS-CDMA Detectors in Blind Space-Time RAKE Receivers for Fading Channels with Delay Spreads Approaching a Symbol's Duration," *IEEE Intl. Conf. Acoustics,Speech & Signal Processing*, vol. 3, pp. 2625–2628, 2002.

[9] J. Litva and T. K.-Y. Lo, *Digital Beamforming in Wireless Communications.* Boston, Mass: Artech House, 1994.

[10] M. D. Zoltowski and J. Ramos, " Blind Adaptive Beamforming for CDMA Based PCS Cellular," *Asilomar Conference*, pp. 378–382, 1995.

[11] M. D. Zoltowski and J. Ramos, " Blind Multi-User Access Interference Cancellation for CDMA Based PCS/Cellular Using Antenna Arrays," *IEEE Intl. Conf. Acoustics,Speech & Signal Processing*, pp. 2730–2733, 1996.

[12] M. D. Zoltowski, Y. F. Chen, and J. Ramos, " Blind 2D RAKE Receivers Based on Space-Time Adaptive MVDR Processing for IS-95 CDMA System," *IEEE Military Communications Conf.*, pp. 618–622, 1996.

[13] S. Verdu, *Multiuser Detection.* New York: Cambridge University Press, 1998.

[14] T. S. Rappaport, *Wireless Communications:Principles and Practice.* Upper Saddle River, N.J.: Prentice Hall PT, 1996.

[15] S. K. Cheng, *Lecture Notes,ELE*343 *Fall* 1999, *Wireless Communication.* Clear Water Bay ,H.K.: The Hong Kong University of Science and Technology, 1999.

[16] Y. F. Chen and M. D. Zoltowski, " Convergence Analysis and Tracking Ability of Reduced Dimension Blind Space-Time Rake Receivers for DS-CDMA," *IEEE Vehicular Technology Conference*, pp. 2333–2337, 1998.

[17] S. Mudulodu and A. Paulraj, " A Blind Multiuser Receiver for the CDMA Downlink," *IEEE Intl. Conf. Acoustics,Speech & Signal Processing*, pp. 2933–2936, 2000.

[18] J. Ramos, M. D. Zoltowski, and H. Liu, " Low-Complexity Space-Time Processor for DS-CDMA Communications," *IEEE Trans. Signal Processing*, vol. 48, pp. 39–52, Jan. 2000.

[19] D. A. Pados and S. N. Batalama, " Joint Space-Time Auxiliary-Vector Filtering for DS/CDMA Systems with Antenna Arrays," *IEEE Trans. Communications*, pp. 1406–1415, 1999.

[20] S. Haykin, *Communication Systems.* New York: Wiley, 1998.

[21] B. Suard, A. Naguib, G. Xu, and T. Kailath, " Performance Analysis of CDMA Mobile Communication Systems Using Antenna Arrays," *IEEE Intl. Conf. Acoustics,Speech & Signal Processing*, vol. 6, pp. 153–156, 1993.

[22] Y. F. Chen and M. D. Zoltowski, " Blind RLS Based Space-Time Adaptive 2-D RAKE Receivers for DS-CDMA Communication Systems," *IEEE Trans. Signal Processing*, vol. 48, pp. 2145–2150, July 2000.

[23] J. Ramos and M. D. Zoltowski, " Reduced Complexity Blind 2D RAKE Receiver for CDMA," *IEEE Signal Processing Workshop on Statistical Signal & Array Processing*, pp. 502–505, 1996.

[24] J. M. Ortega, *Matrix Theory : a second course.* New York: Plenum, 1987.

[25] D. C. Lay, *Linear Algebra And Its Applications,second edition.* New York: Addison-Wesley, 1997.

Appendix A

Generalized Eigenvalue Problem

A.1 Standard Eigenvalue Problem

Given an $n \times n$ square matrix $\mathbf{A}$, an eigenvector is a nonzero vector $\mathbf{x}$ such that $\mathbf{Ax} = \lambda\mathbf{x}$ for some scalar λ. A scalar λ is called an eigenvalue of $\mathbf{A}$ if there is a non-trivial solution $\mathbf{x}$ of $\mathbf{Ax} = \lambda\mathbf{x}$; such an $\mathbf{x}$ is called an eigenvector corresponding to λ.

Reformulate the equation $\mathbf{Ax} = \lambda\mathbf{x}$, it can be expressed as:

$$(\mathbf{A} - \lambda\mathbf{I})\mathbf{x} = 0 \tag{A.1}$$

A.2 Generalized Eigenvalue Problem

If the identity matrix $\mathbf{I}$ is replaced by a square matrix $\mathbf{B}$ with some other properties in Eq.(A.1), the equation becomes

$$(\mathbf{A} - \lambda\mathbf{B})\mathbf{x} = 0 \tag{A.2}$$

With different properties of matrix $\mathbf{A}$ and $\mathbf{B}$, there are some properties of the solving method of Eq.(A.2).

Case 1 :

If **B** is invertible, Eq.(A.2) will be expressed as,

$$(\mathbf{B}^{-1}\mathbf{A})\mathbf{x} = \lambda\mathbf{x} \tag{A.3}$$

The equation has the same form as Eq.(A.1).

Case 2 :

If **A** is invertible and **B** is non-invertiable, Eq.(A.2) can be expressed as the form like case 1 as follows

$$\begin{aligned}(\mathbf{A} - \lambda\mathbf{B})\mathbf{x} &= 0 \\ \mathbf{A}\mathbf{x} &= \lambda\mathbf{B}\mathbf{x} \\ \frac{1}{\lambda}\mathbf{A}\mathbf{x} &= \mathbf{B}\mathbf{x} \\ (\frac{1}{\lambda})\mathbf{x} &= (\mathbf{A}^{-1}\mathbf{B})\mathbf{x} \end{aligned} \tag{A.4}$$

The equation becomes the form like Eq.(A.1).Since **B** is singular, $\mathbf{A}^{-1}\mathbf{B}$ is singular and has at least one zero eigenvalue μ, which means λ is infinite.

Case 3 :

From [24], if both **A** and **B**, of size $n \times n$ are Hermitian, and **B** is positive definite,the generalized eigenvalue problem Eq.(A.2) has n real eigenvalues and n corresponding linearly independent eigenvectors that can be chosen to be orthogonal in the inner product $(\mathbf{x},\mathbf{y}) = \mathbf{x}'\mathbf{B}\mathbf{y}$, where $(.)'$ is the conjugate transpose.Moveover,if **A** is positive definite, the eigenvalues are all positive.

When we find the beamforming weight vector **w** to maximize the SINR ratio, the solution is the largest generalized eigenvector of the matrix pencil pair $(\widehat{\mathbf{K}}_i^{(S+I+N)}, \widehat{\mathbf{K}}_i^{(I+N)})$.

This is because in the expression of SINR ratio,

$$
\begin{aligned}
SINR &= \frac{\mathbf{w}^H\{\widehat{\mathbf{K}}_i^{(S+I+N,ESO)} - \widehat{\mathbf{K}}_i^{(I+N,ESO)}\}\mathbf{w}}{\mathbf{w}^H\widehat{\mathbf{K}}_i^{(I+N,ESO)}\mathbf{w}} \\
&= \frac{\mathbf{w}^H\widehat{\mathbf{K}}_i^{(S+I+N,ESO)}\mathbf{w}}{\mathbf{w}^H\widehat{\mathbf{K}}_i^{(I+N,ESO)}\mathbf{w}} - 1
\end{aligned}
$$

we have to find $\mathbf{w}$ such that it maximizes the numerator $\mathbf{w}^H\widehat{\mathbf{K}}_i^{(S+I+N)}\mathbf{w}$ and minimizes the denominator $\mathbf{w}^H\widehat{\mathbf{K}}_i^{(I+N)}\mathbf{w}$ simultaneously.

In the simple case, if we have a quadratic form $Q(\mathbf{x}) = \mathbf{x^T A x}$, where $(.)^T$ means transpose operation ,$\mathbf{A}$ is an $n \times n$ symmetric matrix, there exists an orthogonal transform $\mathbf{x} = \mathbf{P y}$ such that,

$$
\begin{aligned}
Q(\mathbf{x}) &= \mathbf{x^T A x} \\
&= Q(\mathbf{y}) \\
&= \mathbf{y^T P^T A P y} \\
&= \mathbf{y^T P^{-1} A P y}, \ (\because \mathbf{P^T P = I}) \\
&= \mathbf{y^T D y}
\end{aligned}
\tag{A.5}
$$

where $\mathbf{A} = \mathbf{PDP}^{-1}$, the columns of $\mathbf{P}$ are the eigenvectors of $\mathbf{A}$ and the diagonal matrix $\mathbf{D}$ contains the corresponding eigenvalues in the diagonal entries.

Therefore, in this simple case, the largest value of $Q(\mathbf{x})$ is the largest eigenvalue λ_{max} of $\mathbf{A}$ and the corresponding $\mathbf{x} = \mathbf{v}_{max}$ and the minimum value of $Q(\mathbf{x})$ is the smallest eigenvalue λ_{min} of $\mathbf{A}$ and the corresponding $\mathbf{x} = \mathbf{v}_{min}$.

That is ,$\mathbf{A}$ can be expressed as , $\mathbf{A} = \lambda_{max}\mathbf{v}_{max}\mathbf{v}_{max}^T + \cdots + \lambda_i\mathbf{v}_i\mathbf{v}_i^T + \cdots + \lambda_{min}\mathbf{v}_{min}\mathbf{v}_{min}^T$, where λ_i is the eigenvalues of $\mathbf{A}$ with the corresponding eigenvectors $\mathbf{v}_i$.

The above mentioned mathematical details are in Lay [25].

Therefore we have to find the largest generalized eigenvector of the matrix pencil pair $(\widehat{\mathbf{K}}_i^{(S+I+N)}, \widehat{\mathbf{K}}_i^{(I+N)})$ so that $\mathbf{w}$ can maximize the SINR ratio,That

is, finding the largest generalized eigenvector of the following generalized eigenvalue problem.

$$(\widehat{\mathbf{K}}_i^{(S+I+N)} - \lambda \widehat{\mathbf{K}}_i^{(I+N)})\mathbf{w} = 0 \tag{A.6}$$